

# Methyl Aluminosilsesquioxanes, Models for Lewis Acidic Silica-Grafted Methyl Aluminum Species

Maria D. Skowronska-Ptasinska,<sup>†</sup> Robbert Duchateau,<sup>\*,†</sup>  
Rutger A. van Santen,<sup>†</sup> and Glenn P. A. Yap<sup>‡</sup>

Dutch Polymer Institute/Schuit Institute of Catalysis, Eindhoven University of Technology,  
P.O. Box 513, 5600 MB Eindhoven, The Netherlands, and University of Ottawa,  
K1N 6N5 Ottawa, Ontario, Canada

Received March 29, 2001

The hydroxysilsesquioxanes (*c*-C<sub>5</sub>H<sub>9</sub>)<sub>7</sub>Si<sub>8</sub>O<sub>12</sub>(OH) (**I**) and (*c*-C<sub>5</sub>H<sub>9</sub>)<sub>7</sub>Si<sub>7</sub>O<sub>9</sub>(OH)<sub>2</sub>OSiMePh<sub>2</sub> (**II**) have been studied as model supports for silica-grafted aluminum alkyl species. Treatment of AlMe<sub>3</sub> with **I** gave polymeric  $\{[(c\text{-C}_5\text{H}_9)_7\text{Si}_8\text{O}_{13}]\text{AlMe}_2\}_n$  (**1a**), which is readily transformed into the corresponding monomeric pyridine adduct,  $\{[(c\text{-C}_5\text{H}_9)_7\text{Si}_8\text{O}_{13}]\text{AlMe}_2\cdot\text{Py}\}$  (**1b**). When AlMe<sub>3</sub> was reacted with **II**, noticeable amounts of the 2:1 product  $\{[(c\text{-C}_5\text{H}_9)_7\text{Si}_7\text{O}_{11}(\text{OSiMePh}_2)](\text{AlMe}_2)_2\}_2$  (**2**) and the Brønsted acidic 1:2 product  $\{[(c\text{-C}_5\text{H}_9)_7\text{Si}_7\text{O}_{11}(\text{OSiMePh}_2)]_2\text{-Al}^-\}\{\text{H}^+\}$  (**III**) were obtained besides the main product of the reaction,  $\{[(c\text{-C}_5\text{H}_9)_7\text{Si}_7\text{O}_{11}(\text{OSiMePh}_2)]\text{AlMe}_2\}_2$  (**3a–c**). The main product is a mixture of three dimeric conformational isomers all with the aluminum methyls *trans* to each other. The difference of the conformers originates from the different orientation of the silsesquioxane ligands. Reaction of the Brønsted acid **III** with AlMe<sub>3</sub> yielded the kinetic product  $\{[(c\text{-C}_5\text{H}_9)_7\text{Si}_7\text{O}_{11}(\text{OSiMePh}_2)]_2\text{Al}_2\text{-Me}_2$  (**4**). The kinetic and thermodynamic stability of the three conformeric methyl aluminosilsesquioxanes  $\{[(c\text{-C}_5\text{H}_9)_7\text{Si}_7\text{O}_{11}(\text{OSiMePh}_2)]\text{AlMe}_2\}_2$  (**3a–c**) and their chemical isomer  $\{[(c\text{-C}_5\text{H}_9)_7\text{Si}_7\text{O}_{11}(\text{OSiMePh}_2)]_2\text{Al}_2\text{Me}_2$  (**4**) has been investigated. Isomerization experiments showed that **3a** isomerizes to **3b**, which subsequently isomerizes to **3c**, affording the thermodynamically most stable mixture with a **3a:3b:3c** ratio of 1:4:4 after 400 h at 76 °C. Isomerization of **3a** to **3b** is considerably faster than from **3b** to **3c**. Direct conversion of **3a** into **3c** was not observed. Complex **4** slowly isomerizes into **3c**, which consecutively isomerizes into the thermodynamic most stable isomeric mixture (1000 h at 76 °C, *E*<sub>a</sub> = 117 kJ·mol<sup>-1</sup>). Treating Cp<sub>2</sub>ZrMe<sub>2</sub> with the Brønsted acid **III** gave clean transfer of a silsesquioxane ligand to zirconium, yielding  $[(c\text{-C}_5\text{H}_9)_7\text{Si}_7\text{O}_{11}(\text{OSiMePh}_2)]\text{ZrCp}_2$  (**5**). The methyl aluminosilsesquioxanes **1a** and **2–4** are not Lewis acidic enough to effectively abstract a substituent X from Cp<sub>2</sub>ZrX<sub>2</sub> (X = Me, CH<sub>2</sub>Ph, Cl). Though, **3a–c** and **4** definitely interact with Cp<sub>2</sub>ZrX<sub>2</sub>. Dependent on the substituent X, the zirconocene can accelerate the rate of isomerization over 2 orders of magnitude (**3a**, 1.5 h; **4**, 8 h at 76 °C). Surprisingly, complex **4** also reacts with the strongly Lewis acidic B(C<sub>6</sub>F<sub>5</sub>)<sub>3</sub>. As soon as all **4** has been converted into **3a–c**, the accelerating effect stops, which demonstrates that Lewis acids have no effect on the isomerization of **3a–c**. Complexes **2**, **3a**, **3c**, **4**, and **5** have been structurally characterized.

## Introduction

The development of well-defined homogeneous olefin polymerization catalysts has reached the point that these systems are becoming commercially attractive.<sup>1</sup> Regardless of the excellent properties of these catalysts, their industrial applicability would be limited if they could not be adapted to run in existing commercial

processes. Most industrial processes (bulk monomer, slurry, and gas-phase) require heterogeneous catalysts,<sup>2</sup> which implies that the homogeneous catalyst should be immobilized on an insoluble support.<sup>3</sup>

Homogeneous catalysts that are activated with methylalumoxane (MAO) and supported on inorganic oxides, predominately silicas, form the vast majority of heterogeneous single-site catalysts.<sup>3,4</sup> Commonly, the aluminum cocatalyst is supported prior to the transition metal catalyst precursor. A number of techniques are

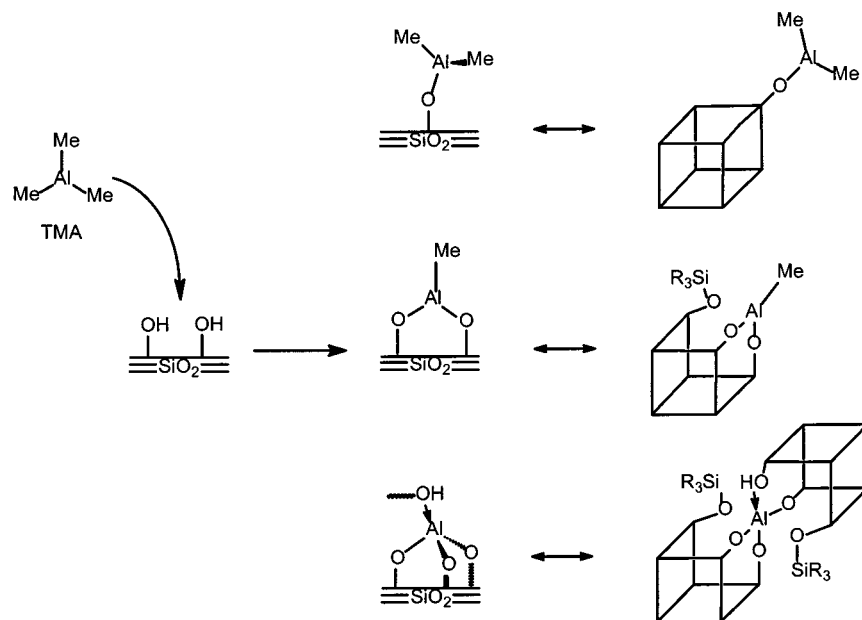
\* Corresponding author. Tel: +31 40 2474918. Fax: +31 40 2455054. E-mail: R.Duchateau@tue.nl.

<sup>†</sup> Eindhoven University of Technology.

<sup>‡</sup> University of Ottawa.

(1) (a) Resconi, L.; Cavallo, L.; Fait, A.; Piemontesi, F. *Chem. Rev.* **2000**, *100*, 1253–1345. (b) Alt, H.; Köppl, A. *Chem. Rev.* **2000**, *100*, 1205–1222. (c) Coates, G. W. *Chem. Rev.* **2000**, *100*, 1223–1252. (d) Dietrich, U.; Hackmann, M.; Rieger, B.; Klinga, M.; Leskelä, M. *J. Am. Chem. Soc.* **1999**, *121*, 4348–4355. (e) Leclerc, M. K.; Waymouth, R. M. *Angew. Chem., Int. Ed.* **1998**, *37*, 922–925. (f) Müller, C.; Lilje, D.; Kristen, M. O.; Jutzi, P. *Angew. Chem., Int. Ed.* **2000**, *39*, 789–792.

(2) For example see: (a) Sinn, H.; Kaminsky, W. *Adv. Organomet. Chem.* **1980**, *18*, 99. (b) Tait, P. T. *Comput. Polym. Sci.* **1989**, *4*, 1. (c) Xie, T.; McAuley, K. B.; Hsu, J. C. C.; Bacon, D. W. *Ind. Eng. Chem. Res.* **1994**, *33*, 449–479. (d) Marsden, C. E. *Plast., Rubber Compos. Process. Appl.* **1994**, *21*, 193–200. (e) Hungenberg, K. D.; Kerth, J.; Langhauser, F.; Marczinke, B.; Schlund, R. In *Ziegler Catalysts*; Fink, G., Mühlhaupt, R., Brintzinger, H. H., Eds.; Springer-Verlag: New York, 1995; Chapter 20.

**Scheme 1. Modeling Surface Aluminum-Siloxy Species with Aluminosilsesquioxanes**

used to produce immobilized alumoxanes.<sup>3</sup> The earliest routes consisted of fixing commercially available MAO to the support.<sup>4,5</sup> An attractive alternative route to generate supported alumoxanes is in situ hydrolysis of trimethylaluminum (TMA) with hydrated silica.<sup>6</sup>

Silicas have also been modified with aluminum alkyls as passivating and/or compatibilizing agents. Not only have homogeneous (co)catalysts been physisorbed onto such carrier materials but also these modified supports have been used to chemically link hydroxyl or amine functionalized (co)catalysts.<sup>7</sup>

On reaction with TMA, the different surface silanol functionalities present on the amorphous oxides will invariably yield various surface aluminum sites with different properties. Investigating the formation and character of surface aluminum species as well as their interaction with the (pre)catalysts may give better insight into their role in olefin polymerization catalysis. However, such studies are dramatically hampered by the heterogeneity of these systems.<sup>8</sup> Recently, with the

aid of silsesquioxanes as model supports, various reactions taking place at silica surface silanol sites have been mimicked successfully.<sup>9,10</sup> With silsesquioxanes, we intended to gain a better understanding of the interaction of aluminum alkyl species with silica surface silanols.

We here report the synthesis and characterization of Lewis acidic methyl-aluminosilsesquioxane complexes that mimic surface aluminum methyl species formed upon treating hydroxylated silicas with trimethylaluminum (Scheme 1). Furthermore, the kinetic and thermodynamic stability of these complexes as well as their reactivity toward zirconocene complexes will be discussed.

**Results and Discussion.**

**Synthesis of Methyl Aluminosilsesquioxanes.** As a start, we investigated the reactivity of trimethylaluminum (TMA) with isolated silanol functionalities by treating the monosilanol (*c*-C<sub>5</sub>H<sub>9</sub>)<sub>7</sub>Si<sub>8</sub>O<sub>12</sub>(OH) (**I**) with TMA. Reaction of **I** with an equimolar amount of TMA in toluene affords aluminosilsesquioxane {[(*c*-C<sub>5</sub>H<sub>9</sub>)<sub>7</sub>Si<sub>8</sub>O<sub>13</sub>AlMe<sub>2</sub>]<sub>n</sub>} (**1a**, Scheme 2). Unlike most metal complexes containing ligand **I**,<sup>10b</sup> compound **1a** is completely insoluble in hexane and forms a gel in toluene, indicating that **1** has a polymeric structure.<sup>11</sup> Upon addition of pyridine (1 equiv) to a suspension of **1a** in hexane, a clear solution is formed from which the corresponding monomeric pyridine adduct [(*c*-C<sub>5</sub>H<sub>9</sub>)<sub>7</sub>Si<sub>8</sub>O<sub>13</sub>AlMe<sub>2</sub>Py] (**1b**, Scheme 2) crystallizes (−30 °C) as fine colorless needles.

The NMR spectra of **1a** and **1b** show the characteristic resonances for the C<sub>3</sub> symmetric silsesquioxane cage structure (<sup>13</sup>C, 1:3:3 ratio for CH–C<sub>5</sub>H<sub>9</sub>; <sup>29</sup>Si, 1:3:3:1 ratio) and the high-field resonance for the aluminum methyl (**1a**: <sup>1</sup>H, −0.13 ppm; <sup>13</sup>C, −9.31 ppm; **1b**: <sup>1</sup>H, −0.25 ppm; <sup>13</sup>C, −9.03 ppm).

Silsesquioxane (*c*-C<sub>5</sub>H<sub>9</sub>)<sub>7</sub>Si<sub>7</sub>O<sub>9</sub>(OH)<sub>2</sub>OSiMePh<sub>2</sub> (**II**) represents a vicinal disilanol site, abundantly present in hydroxylated silicas (Scheme 1).<sup>3b</sup> The selectivity of the

(3) (a) Hlatky, G. G. *Coord. Chem. Rev.* **1999**, *181*, 243–296. (b) Chien, J. C. W. *Top. Catal.* **1999**, *7*, 23–36. (c) Hlatky, G. G. *Chem. Rev.* **2000**, *100*, 1347–1376.

(4) (a) Chien, J. C. W.; He, D. *J. Polym. Sci., A: Polym. Chem.* **1991**, *29*, 1603–1607. (b) Collins, S.; Kelly, W. M.; Holden, D. A. *Macromolecules* **1992**, *25*, 1780–1785. (c) Soga, K.; Kaminaka, M. *Makromol. Chem., Rapid Commun.* **1992**, *13*, 221–224. (d) Soga, K.; Kaminaka, M. *Makromol. Chem.* **1993**, *194*, 1745–1755. (e) Kaminsky, W.; Renner, F. *Makromol. Chem., Rapid Commun.* **1993**, *14*, 239–243. (f) Janiak, C.; Rieger, B. *Angew. Makromol. Chem.* **1994**, *215*, 47–57. (g) Sacchi, M. C.; Zucchi, D.; Titto, I.; Locatelli, P.; Dall'Occo, T. *Macromol. Rapid Commun.* **1995**, *16*, 581–590. (h) Kamfjord, T.; Wester, T. S.; Rytter, E. *Macromol. Rapid Commun.* **1998**, *19*, 505–509.

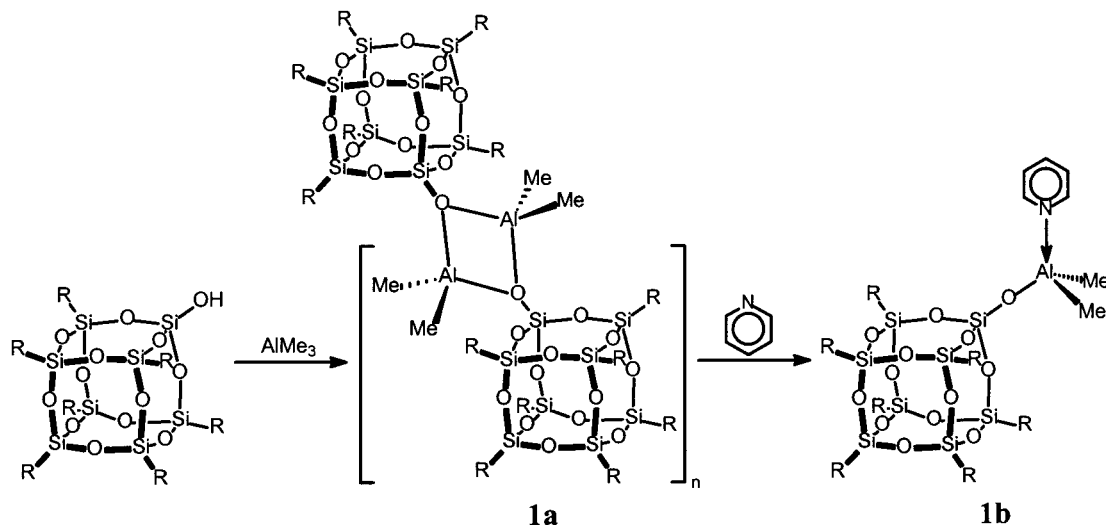
(5) (a) Welborn, H. C. U.S. Patent 4,808,561, 1989. (b) Kioka, M.; Kashiwa, N. U.S. Patent 4,874,734, 1989. (c) Takahashi, T. U.S. Patent 5,026,797, 1991.

(6) (a) Chang, M. U.S. Pat. 5,008,228, 1991. (b) Tsutsui, T.; Ueda, T. U.S. Patent 5,234,878, 1993. (c) Gürtzgen, S. U.S. Patent 5,446,001, 1995. (d) Herrmann, H. F.; Bachmann, B.; Spaleck, W. Eur. Pat. Appl. 578,838, 1994. (e) Becker, R.-J.; Rieger, R. Eur. Pat. Appl. 763,546, 1997. (f) Becker, R.-J.; Gürtzgen, S.; Kutschera, D. U.S. Patent 5,534,474, 1996. (g) Kutschera, D.; Rieger, R. U.S. Patent 5,789,332, 1998.

(7) (a) Nakajima, M.; Kanewaza, S.; Takeshi, I. Japanese Kokai H7-268029, 1995. (b) Jacobsen, G. B.; Wijkens, P.; Jastrzebski, J. T. B. H.; van Koten, G. U.S. Patent 5,834,393, 1998.

(8) Anwender, R.; Palm, C.; Groeger, O.; Engelhardt, G. *Organometallics* **1998**, *17*, 2027–2036.

**Scheme 2. Preparation of the Polymeric Methyl Aluminosilsesquioxane 1a and the Corresponding Monomeric Pyridine Adduct 1b**



apparently simple stoichiometric reaction of **II**<sup>12</sup> with trimethylaluminum (TMA) strongly depends on the reaction conditions. When disilanol **II** was added to a cooled ( $-80\text{ }^{\circ}\text{C}$ ) toluene solution of TMA, various products were formed. Each product was fully characterized by multinuclear NMR techniques, and if possible the molecular structure was elucidated by an X-ray single-crystal structure analysis. The first complex to crystallize from hexane was the dimeric bis(dimethylaluminum)silsesquioxane,  $\{[(c\text{-C}_5\text{H}_9)_7\text{Si}_7\text{O}_{11}(\text{OSiMePh}_2)]\text{-}(\text{AlMe}_2)_2\}_2$  (**2**, Scheme 3), in which one silsesquioxane has reacted with 2 equiv of TMA. The main product of the reaction is a mixture of conformational isomers of  $\{[(c\text{-C}_5\text{H}_9)_7\text{Si}_7\text{O}_{11}(\text{OSiMePh}_2)]\text{AlMe}_2\}_2$  (**3a–c**, Scheme 3). Noticeable ( $\sim 10\%$ ) amounts of the Brønsted acid  $\{[(c\text{-C}_5\text{H}_9)_7\text{Si}_7\text{O}_{11}(\text{OSiMePh}_2)]_2\text{Al}^-\}\{\text{H}^+\}$  (**III**, Scheme 3), formed by the reaction of  $\text{AlMe}_3$  with 2 equiv of **II**,<sup>10d,e</sup> were also isolated. Attempts to produce **2** in higher yield by reacting **II** with 2 equiv of TMA failed, as only oily product mixtures were obtained. The fact that **2** and **3a–c** do not undergo protonolysis with the Brønsted acidic aluminosilsesquioxane **III** indicates effective

shielding of the methyl substituents in the dimers **2** and **3a–c**.

When the order of addition was reversed and TMA was added to a cooled ( $-80\text{ }^{\circ}\text{C}$ ) toluene solution containing **II**, only traces of **2** or **III** were formed. The isolated product obtained after crystallization from hexane consisted of  $\{[(c\text{-C}_5\text{H}_9)_7\text{Si}_7\text{O}_{11}(\text{OSiMePh}_2)]\text{AlMe}_2\}_2$  (**3a–c**) in an 8:1:1 ratio.

**Solution and Solid State Structure of 2 and 3a–c.** Complex **2** consists of a  $C_i$  symmetric structure formed by two  $\mu\text{-O}$ -bridged silsesquioxanes and four dimethylaluminum fragments (Figure 1). Like many aluminum alkoxides,<sup>13</sup> the bridging siloxy functionalities form planar four-centered rings with the aluminum centers. The aluminum atoms are tetrahedrally surrounded by two methyl groups and two planar (sum of angles:  $358.7(10)^\circ$ ) oxygen atoms. The  $\text{Al}-\text{CH}_3$  and  $\text{Al}-\text{OSi}\equiv$  distances (Table 1) are comparable to those of methyl aluminum alkoxides.<sup>13</sup> As a result of the  $\sigma+\pi$  bonding of O1 and O7 to the aluminum center, the  $\text{Si}1-\text{O}1$  (1.641(2) Å) and  $\text{Si}5-\text{O}7$  (1.646(2) Å) distances are clearly elongated with respect to the average  $\text{Si}-\text{O}$  distance (1.618(2) Å) in **2**, although they are still well within the wide range of  $\text{Si}-\text{O}$  distances observed for silsesquioxane compounds.<sup>9,10</sup> The molecular structure of **2** (Figure 1) shows the presence of two different types (*exo*, *endo*) of methyl groups. The single  $\text{Al}-\text{CH}_3$  resonance in the  $^1\text{H}$  NMR spectrum ( $25\text{ }^{\circ}\text{C}$ , toluene- $d_6$ ) of **2** therefore indicates highly fluxional behavior in solution at room temperature. The low Gibbs free energy of rotation of this fluxional behavior ( $\Delta G^\ddagger_{\text{TC}} = 48\text{ kJ}\cdot\text{mol}^{-1}$ ,  $T_c = -55\text{ }^{\circ}\text{C}$ ) suggests that complete dissociation of **2** is not necessary for rotation to take place. The  $^{13}\text{C}$  and  $^{29}\text{Si}$  NMR spectra of **2** show the expected pattern for the  $C_s$  symmetric silsesquioxane framework consisting of five cyclopentyl- $\text{CH}$  resonances (2:2:1:1:1 ratio), one  $\text{SiMePh}_2$ , and five framework ( $=\text{O}$ ) $_3\text{Si}(c\text{-C}_5\text{H}_9)$  (2:2:1:1:1 ratio) signals.

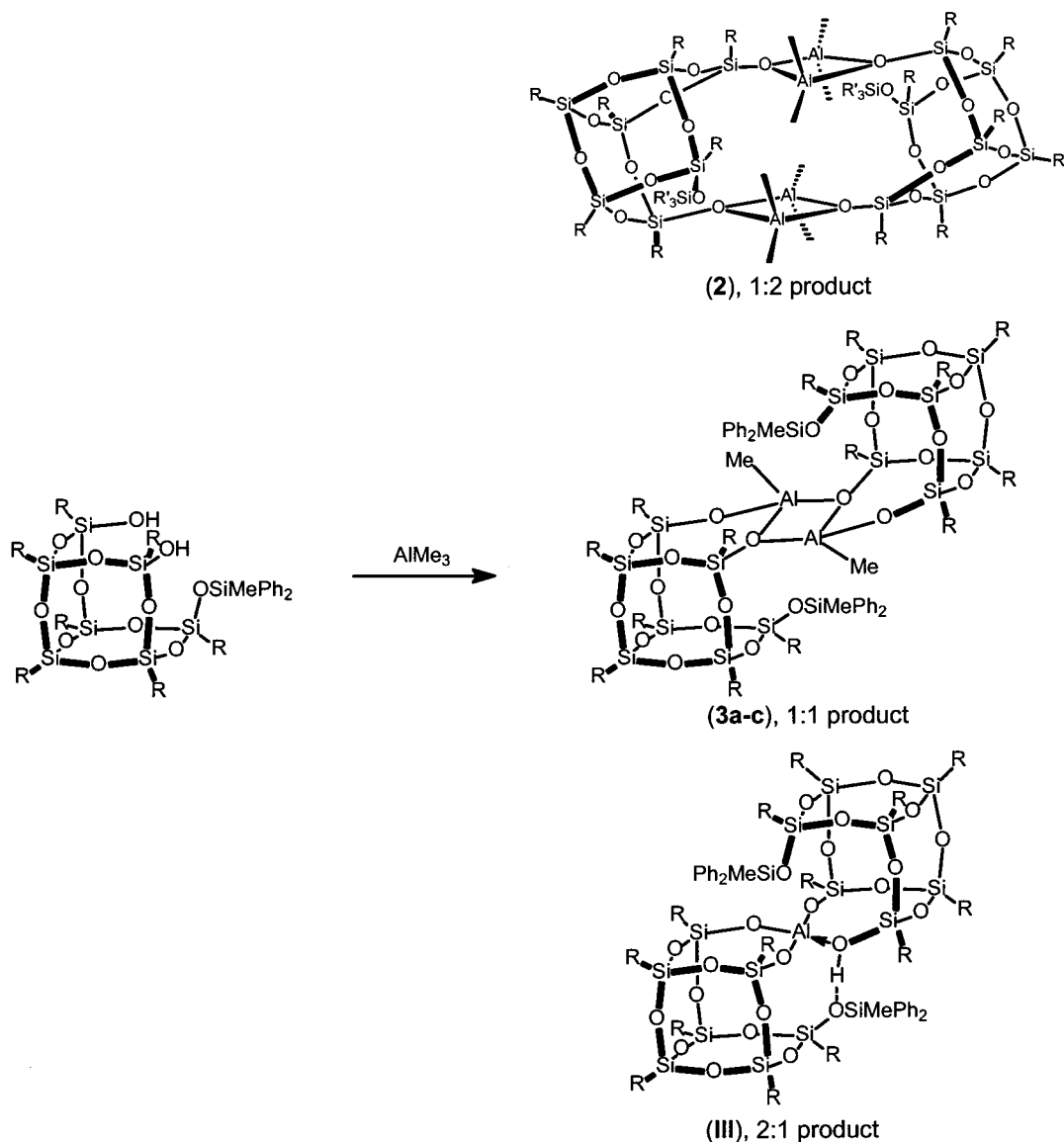
As expected, **3a–c** are dimeric with both bridging and  $\sigma$ -bonded siloxy units (Figure 2).<sup>13</sup> In these dimers the aluminum methyl groups can be either *cis* or *trans* to each other, and each  $C_s$  symmetric silsesquioxane ligand can adopt two different orientations, giving six possible

(9) (a) Feher, F. J.; Newman, D. A.; Walzer, J. F. *J. Am. Chem. Soc.* **1989**, *111*, 1741–1748. (b) Feher, F. J.; Newman, D. A. *J. Am. Chem. Soc.* **1990**, *110*, 1931–1936. (c) Feher, F. J.; Weller, K. J. *Organometallics* **1990**, *9*, 2638–2640. (d) Feher, F. J.; Blanski, R. L. *J. Chem. Soc., Chem. Commun.* **1990**, 1614–1616. (e) Feher, F. J.; Walzer, J. F.; Blanski, R. L. *J. Am. Chem. Soc.* **1991**, *113*, 3618–3619. (f) Feher, F. J.; Budzichowski, T. A. *Polyhedron* **1995**, *14*, 3239–3253. (g) Liu, J.-C. *Appl. Organomet. Chem.* **1999**, *13*, 295–302.

(10) (a) Duchateau, R.; Abbenhuis, H. C. L.; van Santen, R. A.; Meetsma, A.; Thiele, S. K.-H.; van Tol, M. F. H. *Organometallics* **1998**, *17*, 5663–5673. (b) Duchateau, R.; Cremer, U.; Harmsen, R. J.; Mohamud, S.; Abbenhuis, H. C. L.; van Santen, R. A.; Meetsma, A.; Thiele, S. K.-H.; van Tol, M. F. H.; Kranenburg, M. *Organometallics* **1999**, *18*, 5447–5459. (c) Duchateau, van Santen, R. A.; Yap, G. P. A. *Organometallics* **2000**, *19*, 809–816. (d) Duchateau, R.; Harmsen, R. J.; Abbenhuis, H. C. L.; van Santen, R. A.; Meetsma, A.; Thiele, S. K.-H.; Kranenburg, M. *Chem. Eur. J.* **1999**, *5*, 3130–3135. (e) Skowronska-Ptasinska, M. D.; Duchateau, R.; van Santen, R. A.; Yap, G. P. A. *Eur. J. Inorg. Chem.* **2001**, 133–137.

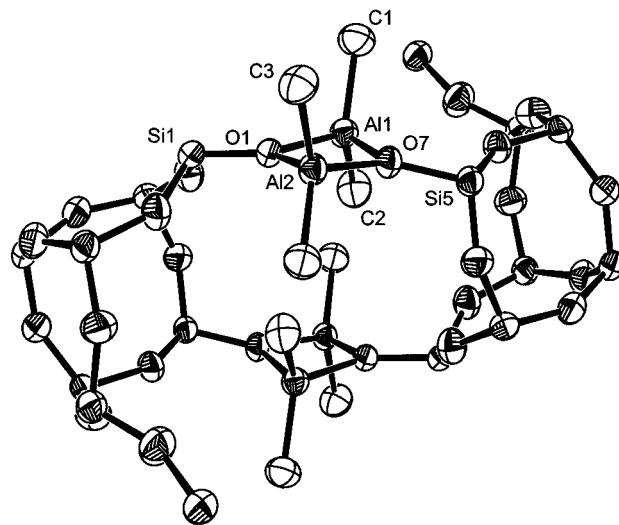
(11) Although dimers and oligomeric ring structures are more common for alkyl aluminum alkoxides, polymeric structures have been reported for corresponding alkyl aluminum thiolates. (a) Oliver, J. P.; Kumar, R. *Polyhedron* **1990**, *9*, 409–427. (b) Dickson, P. M.; Oliver, J. P. *J. Organomet. Chem.* **2000**, *597*, 105–110.

(12) (a) This silsesquioxane is similar to the earlier reported  $(c\text{-C}_5\text{H}_9)_7\text{Si}_7\text{O}_9(\text{OH})_2\text{OSiMe}_3$  albeit that complexes of **II** have a higher tendency to crystallize. (b) Reference 9a.

**Scheme 3. Products Formed upon Reacting II with an Equimolar Amount of TMA**

structures in total. The obtained product mixture exclusively consists of the three conformational isomers, **3a**, **3b**, and **3c**, all with the aluminum methyl substituents *trans* to each other. The corresponding *cis*-isomers were not observed. Recrystallization of saturated hexane solutions of **3a–c** afforded crystals of **3a** and **3c** suitable for an X-ray structure analysis (Figure 2). Unfortunately, no single crystals of **3b** could be obtained.

In both conformers **3a** and **3c** two bridging siloxy functionalities form a four-membered ring with two  $\text{AlMe}$  fragments. The second,  $\sigma$ -bonded siloxy group fills the tetrahedral coordination sphere of both aluminas. The different structures of both conformers result from the different orientation of the silsesquioxane fragments. In **3a** both  $\text{SiMePh}_2$  ( $\text{Si8}$ ) substituents are *exo* to the aluminum methyl ( $\text{C1}$ ) groups, while in **3c** the two  $\text{SiMePh}_2$  ( $\text{Si8}$ ) substituents are *endo* with respect to the aluminum methyl ( $\text{C1}$ ) groups. The  $\text{Al–C}$  bonds in **3a** and **3c** are significantly shorter than in **2** (Table 1), suggesting that the metal centers in **3a–c** are more electrophilic than in **2**. This assumption is supported by the large  $\sigma$ -bonded  $\text{Si–O–Al}$  angles (**3a**,  $150.6(15)^\circ$ ; **3c**,  $158.7(4)^\circ$ ), which indicates additional  $\pi$ -donation of

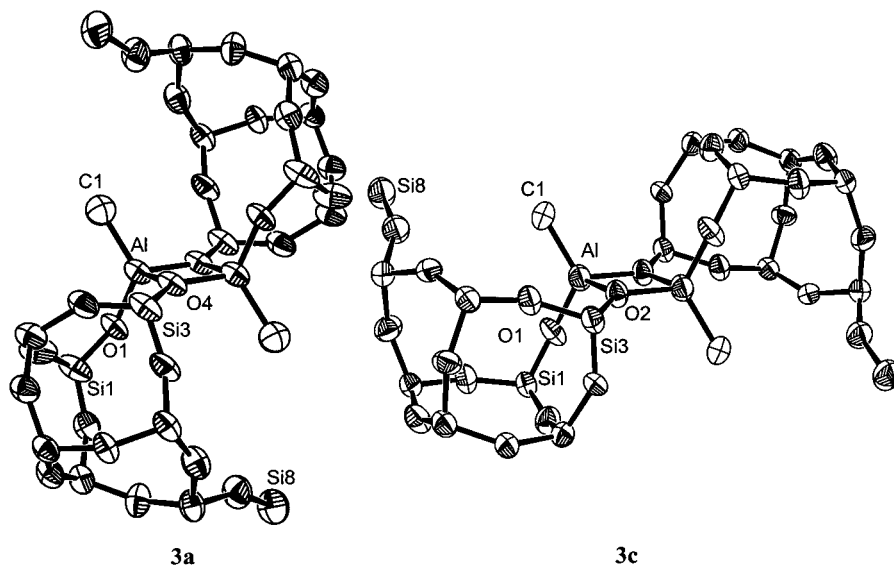


**Figure 1.** ORTEP diagram of the molecular structure of **2**. Thermal ellipsoids are drawn at the 40% probability level. Hydrocarbyl substituents on silicon are omitted for clarity.



**Table 1.** Selected Bond Distances (Å) and Angles (deg) for  $\{[(c\text{-C}_5\text{H}_9)_7\text{Si}_7\text{O}_{11}(\text{OSiMePh}_2)](\text{AlMe}_2)_2\}_2$  (**2**),  $\{[(c\text{-C}_5\text{H}_9)_7\text{Si}_7\text{O}_{11}(\text{OSiMePh}_2)]\text{AlMe}_2\}_2$  (**3a/3c**),  $[(c\text{-C}_5\text{H}_9)_7\text{Si}_7\text{O}_{11}(\text{OSiMePh}_2)]_2\text{Al}_2\text{Me}_2$  (**4**), and  $[(c\text{-C}_5\text{H}_9)_7\text{Si}_7\text{O}_{11}(\text{OSiMePh}_2)]\text{ZrCp}_2$  (**5**)

<b>2</b>	<b>3a</b>	<b>3c</b>	<b>4</b>	<b>5</b>
Al1–O1 = 1.878(2)	Al–O1 = 1.72(2)	Al–O1 = 1.706(6)	Al1–C1 = 1.914(10)	Zr–O1 = 1.994(2)
Al1–O7 = 1.873(2)	Al–O4 = 1.907(8)	Al–O2 = 1.862(5)	Al1–O1 = 1.861(5)	Zr–O7 = 1.995(2)
Al2–O1 = 1.867(2)	Al–O4' = 1.793(8)	Al–O2' = 1.852(5)	Al2–O1 = 1.814(5)	Zr–Ct1 = 2.239(2)
Al2–O7 = 1.855(2)	Al–C1 = 1.898(8)	Al–C1 = 1.899(8)	Al2–O6 = 1.711(6)	Zr–Ct2 = 2.252(2)
Al1–C1 = 1.953(4)	Si1–O1 = 1.55(2)	Si1–O1 = 1.582(5)	Si1–O1 = 1.643(5)	O1–Si1 = 1.603(2)
Al1–C2 = 1.926(4)	Si3–O4 = 1.656(6)	Si3–O2 = 1.649(5)	Si3–O6 = 1.602(6)	O7–Si3 = 1.605(2)
Al2–C3 = 1.960(4)	Si–O <sub>av</sub> = 1.619(7)	Si–O <sub>av</sub> = 1.614(5)	Si–O <sub>av</sub> = 1.611(6)	Si–O <sub>av</sub> = 1.625(2)
Al2–C4 = 1.946(4)				
Si1–O1 = 1.641(2)				
Si5–O7 = 1.646(2)				
Si–O <sub>av</sub> = 1.618(2)				
O1–Al1–O7 = 82.36(10)	O4–Al–O4' = 83.3(3)	O2–Al–O2' = 83.8(2)	O1–Al1–O1' = 82.0(3)	O1–Zr–O7 = 97.23(8)
O1–Al2–O7 = 83.12(10)	Al–O4–Al' = 96.7(4)	Al–O2–Al' = 96.2(2)	O1–Al1–C1 = 110.2(4)	O1–Zr–Cg1 = 105.67(8)
Al1–O1–Al2 = 96.32(10)	O1–Al–O4 = 105.7(8)	O1–Al–O2 = 106.9(3)	O1–Al1–C1' = 112.4(4)	O1–Zr–Cg2 = 105.71(8)
Al1–O7–Al2 = 96.90(10)	O1–Al–O4' = 110.9(8)	O1–Al–O2' = 108.2(3)	O1–Al2–O1' = 84.6(3)	O7–Zr–Cg1 = 108.54(8)
C1–Al1–C2 = 119.73(18)	O1–Al–C1 = 121.4(9)	O1–Al–C1 = 122.4(3)	O6–Al2–O6' = 116.2(4)	O7–Zr–Cg2 = 107.36(8)
C3–Al2–C4 = 117.33(18)	O4–Al–C1 = 118.4(8)	O2–Al–C1 = 115.1(4)	O1–Al2–O6 = 111.6(2)	Cg1–Zr–Cg2 = 128.01(8)
Si1–O1–Al1 = 133.75(14)	O4'–Al–C1 = 110.8(7)	O2'–Al–C1 = 113.8(3)	O1–Al2–O6' = 114.4(2)	
Si1–O1–Al2 = 129.89(13)	Si1–O1–Al = 150.6(15)	Si1–O1–Al = 158.7(4)	Si1–O1–Al1 = 132.3(3)	
Si5–O7–Al1 = 124.37(13)	Si3–O4–Al = 135.8(4)	Si3–O2–Al = 126.6(3)	Si1–O1–Al2 = 128.9(3)	
Si5–O7–Al2 = 138.35(14)	Si3–O4–Al' = 126.5(4)	Si3–O2–Al' = 135.5(3)	Si3–O6–Al2 = 146.2(3)	

**Figure 2.** ORTEP diagram of the molecular structures of **3a** and **3c**. Thermal ellipsoids are drawn at the 40% probability level. Hydrocarbyl substituents on silicon are omitted for clarity.

the  $\sigma$ -bonded siloxy units to the electrophilic aluminum center. As in **2**, the bridging oxygens are trigonal planar (sum of angles: **3a**, 359.0(4) $^\circ$ ; **3c**, 358.3(2) $^\circ$ ). The O–Al and O–Si distances of the bridging siloxy groups as well as the average silsesquioxane Si–O bond lengths in **3a/c** are very similar to those in **2**. The NMR spectra of **3a** and **3c** are in agreement with a  $C_2$  symmetric dimeric structure as depicted in Figure 2. The silsesquioxane ligands lost their local ( $C_s$ ) symmetry, giving distinct resonances in both  $^{13}\text{C}$  and  $^{29}\text{Si}$  NMR spectra for the seven inequivalent cyclopentyl-CH and  $\text{O}_3\text{Si}(\text{C}_5\text{H}_9)$ , respectively. The  $^1\text{H}$  NMR spectra of **3a** and **3c** show one  $\text{AlCH}_3$  (**3a**,  $\delta$  –0.23 ppm; **3c**,  $\delta$  –0.35 ppm) and one  $\text{SiCH}_3$  (**3a**,  $\delta$  0.94 ppm; **3c**,  $\delta$  0.92 ppm) singlet.

Although **3b** could not be crystallized, removal of **3a** and **3c** by fractional crystallization left a product mixture consisting of 90% of **3b**. The  $^1\text{H}$  NMR spectrum of **3b** shows two sets of equi-intense singlets for the  $\text{AlCH}_3$  ( $\delta$  –0.08, –0.10 ppm) and  $\text{SiCH}_3$  ( $\delta$  1.04, 0.94

ppm) substituents, respectively, resulting from an asymmetric dimer with inequivalent aluminum centers. Correspondingly, two  $\text{AlCH}_3$ , two  $\text{Si}(\text{CH}_3)\text{Ph}_2$ , and 14 equi-intense cyclopentyl-CH resonances are observed in the  $^{13}\text{C}$  NMR spectrum, while the  $^{29}\text{Si}$  NMR spectrum shows two  $\text{SiMePh}_2$  and 14 equi-intense  $(\equiv\text{O})_3\text{Si}(\text{C}_5\text{H}_9)$  resonances. This agrees with a dimeric structure as depicted in Figure 3, in which the methyl substituents are *trans* to each other and one of the methyl groups is *endo* and the other *exo* with respect to the  $\text{SiMePh}_2$  substituents.<sup>14</sup>

**Formation and Reactivity of a Brønsted Acidic Aluminosilsesquioxane.** Reacting highly hydroxylated silicas with aluminum alkyls might result in Brønsted acidic aluminosilicate structures, which in

(13) (a) Oliver, J. P.; Kumar, R. *Polyhedron* **1990**, *9*, 409–427. (b) Taden, I.; Kang, K.-C.; Massa, W.; Spaniol, T. P.; Okuda, J. *Eur. J. Inorg. Chem.* **2000**, 441–445, and references therein.

(14) A force field optimized structure was obtained using a Molecular Mechanics program implemented in the CAChe software.

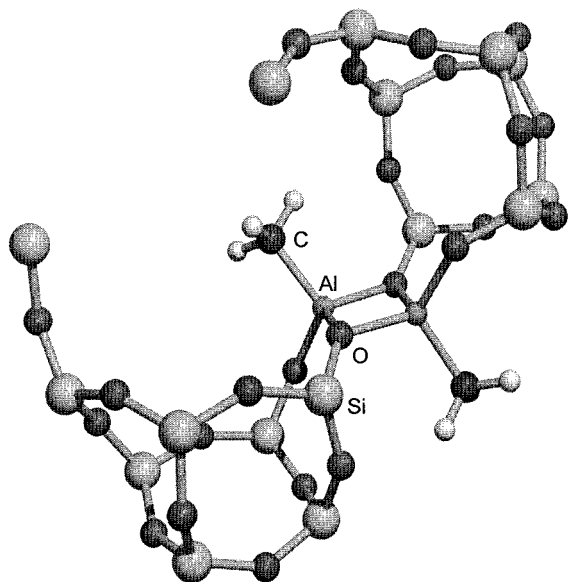


**Figure 3.** Proposed structure of **3b**. Hydrocarbyl substituents on silicon are omitted for clarity.

turn can react further with additional aluminum alkyls. Recently we reported the synthesis and characterization of several aluminosilsesquioxanes that mimic Brønsted acidic aluminosilicate surface sites.<sup>10d,e</sup> For example, the reaction of  $(c\text{-C}_5\text{H}_9)_7\text{Si}_7\text{O}_9(\text{OH})_2\text{OSiMePh}_2$  with 0.5 equiv of  $\text{AlMe}_3$  yielded the Brønsted acid  $\{[(c\text{-C}_5\text{H}_9)_7\text{Si}_7\text{O}_{11}(\text{OSiMePh}_2)_2\text{Al}^-]\{\text{H}^+\}$  (**III**).<sup>10e</sup> Since aluminosilicate sites similar to **III** might initially be formed during grafting of aluminum alkyls onto silica, we are interested in the reactivity of **III** toward TMA.

As expected, TMA is readily protonolyzed by the acidic proton of **III**, affording the novel  $C_2$  symmetric aluminosilsesquioxane,  $[(c\text{-C}_5\text{H}_9)_7\text{Si}_7\text{O}_{11}(\text{OSiMePh}_2)_2\text{Al}_2\text{Me}_2$  (**4**). The molecular structure of **4** was confirmed by single-crystal X-ray analysis (Figure 4). Al1 and Al2 are linked together by two  $\mu$ -bridged siloxy groups (Al1–O1, 1.861(5) Å; Al2–O1 = 1.814(5) Å). The coordination sphere of Al1 is filled by two methyl substituents (Al1–C1, 1.914(10) Å), whereas Al2 coordinates two additional  $\sigma$ -bonded siloxy groups (Al2–O6 = 1.711(6) Å). The Al1–C1 bond (1.914(10) Å) is slightly longer than those in **3a** and **3c**, and the  $\sigma$ -O6–Al2 distance (1.711(6) Å) corresponds well with the  $\sigma$ -O–Al bonds in **3a** and **3c** (Table 1). In agreement with the  $C_2$  symmetric structure of **4**, the  $^1\text{H}$  NMR spectrum of **4** shows one  $\text{SiCH}_3$  ( $\delta$  0.86 ppm) and one high-field  $\text{AlCH}_3$  ( $\delta$  –0.24 ppm) resonance, while the  $^{13}\text{C}$  and  $^{29}\text{Si}$  NMR spectra display seven distinct cyclopentyl-CH, one  $\text{OSiMePh}_2$ , and seven equi-intense  $(\equiv\text{O})_3\text{Si}(\text{C}_5\text{H}_9)$  resonances. Compound **4** is an analogue of  $\{[(c\text{-C}_5\text{H}_9)_7\text{Si}_7\text{O}_{11}(\text{OSiMe}_3)_2\text{Al}^-]\{\text{Li}(\text{THF})_2^+\}$ , obtained by the reaction of  $(c\text{-C}_5\text{H}_9)_7\text{Si}_7\text{O}_9(\text{OH})_2\text{OSiMe}_3$  with 0.5 equiv of  $\text{LiAlH}_4$ . The latter complex can be considered to consist of a  $\text{Li}^+(\text{THF})_2$  fragment stabilized by the anionic  $[(c\text{-C}_5\text{H}_9)_7\text{Si}_7\text{O}_{11}(\text{OSiMePh}_2)_2\text{Al}^-]$ .<sup>10d</sup> However, due to the higher electronegativity of Al (1.6) in comparison with Li (1.0), such an ionic structure is not realistic in the case of complex **4** (vide infra).

**Isomerization of Methyl Aluminosilsesquioxanes.** While stable at room temperature, in 400 h at 76 °C the kinetic mixture of **3a–c**, isolated in an 8:1:1 ratio

after crystallization, converts into the thermodynamic most stable ratio of **3a:3b:3c**  $\approx$  1:4:4 (Figure 5a).

As can be seen from Figure 5a, complex **3a** isomerizes more rapidly into **3b** than **3b** isomerizes into **3c** ( $k_1, k_{-1} > k_2, k_{-2}$ ). Isomerization of **3a–c** can proceed via various mechanisms. However, rehybridization of the aluminum center is required to convert the *exo* and *endo* conformations into each other. Complete dissociation of the dimer is not very likely to occur since the aluminum centers are strongly Lewis acidic. Alternatively, a bridging siloxide could dissociate from one of the aluminum centers, yielding an intermediate with only one coordinatively unsaturated, trigonal-planar aluminum center. Most probably, bridging and terminal siloxy units interchange by a concerted mechanism, forming a TBP-coordinated aluminum site, since the formation of strongly Lewis acidic aluminum intermediates is avoided. On the basis of a molecular mechanics study this mechanism proved feasible and agrees with the observed successive isomerization from **3a**  $\leftrightarrow$  **3b**  $\leftrightarrow$  **3c**. Direct isomerization of **3a** into **3c** cannot be excluded at this point.

Formally, complex **4** consists of a dimer containing a trisiloxaluminum unit  $(\equiv\text{SiO})_3\text{Al}$  and a dimethylaluminum siloxide unit  $(\equiv\text{SiO})\text{AlMe}_2$  and can be seen as a trapped intermediate of the imaginary redistribution reaction  $(\equiv\text{SiO})_3\text{Al} + (\equiv\text{SiO})\text{AlMe}_2 \rightarrow (\equiv\text{SiO})_2\text{Al}(\mu\text{-OSi}\equiv)_2\text{AlMe}_2 \rightarrow \text{Me}(\equiv\text{SiO})\text{Al}(\mu\text{-}\equiv\text{SiO})_2\text{Al}(\text{OSi}\equiv)\text{Me}$ . Such redistribution reactions are widely applied to prepare organoaluminum compounds and are postulated to occur via formation of mixed associates with bridging groups of both components.<sup>15</sup> In the case of **4**, such a redistribution reaction would at the end provide methylaluminumdisiloxides. Indeed, upon heating solutions of **4** in toluene or benzene- $d_6$ , characteristic resonances of **3a**, **3b**, and **3c** slowly appear in the NMR spectra as complex **4** is gradually transformed in a mixture of these isomers (Figure 5b). Continued heating of the mixture yields the thermodynamic mixture of **3a–c** (vide supra). From Figure 5b it can be seen that reaching the thermodynamic equilibrium takes considerably longer (approximately 1000 h) than when starting from **3a** (approximately 400 h, Figure 5a). This originates from the different equilibration rates for **3a**  $\leftrightarrow$  **3b** (fast) and **3b**  $\leftrightarrow$  **3c** (slow) and corresponds with the observation that complex **4** isomerizes (mainly) in **3c**, which consecutively isomerizes only slowly into **3b** and **3a**. However, several mechanisms for the isomerization of **4** into **3a–c** are plausible, and it cannot be excluded that **4** partly isomerizes into **3b/3a** as well. Most probably, isomerization proceeds via a TBP-coordinated aluminum intermediate rather than a strongly Lewis acidic trigonal-planar aluminum site.

The unimolecularity of isomerization is also indicated by kinetic studies carried out by monitoring the isomerization of **4** into **3a–c** by  $^1\text{H}$  NMR spectroscopy in benzene- $d_6$ . The reaction is clearly first order in concentration of **4** over a period of several half-lives (Figure 6). The isomerizations were carried out at different temperatures, and from the Arrhenius plot an activation

(15) For example see: Mole, T.; Jeffery, E. A. In *Organoaluminum Compounds*; Elsevier: Amsterdam, 1972.

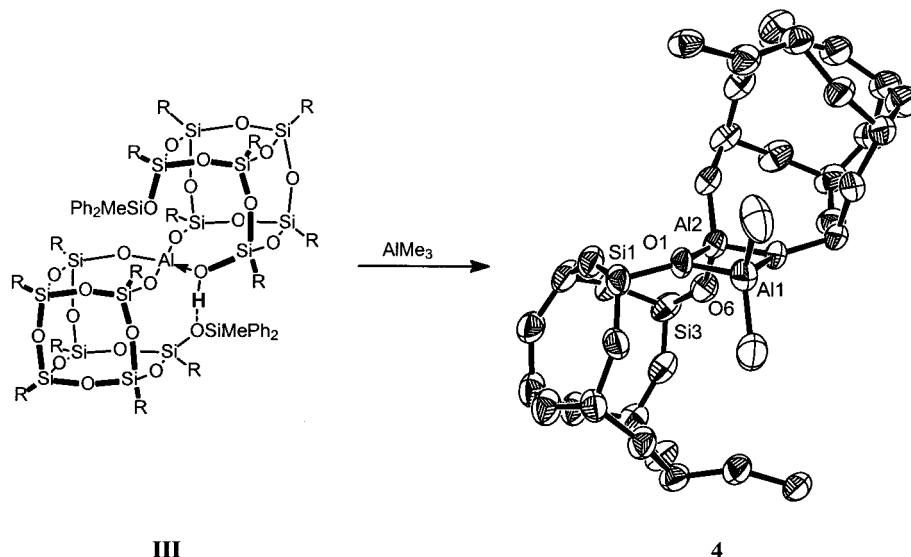


**Figure 4.** Synthesis and ORTEP drawing of  $[(c\text{-C}_5\text{H}_9)_7\text{Si}_7\text{O}_{11}(\text{OSiMePh}_2)_2]\text{Al}_2\text{Me}_2$  (**4**). Thermal ellipsoids are drawn at the 40% probability level. Hydrocarbon substituents on silicon are omitted for clarity.

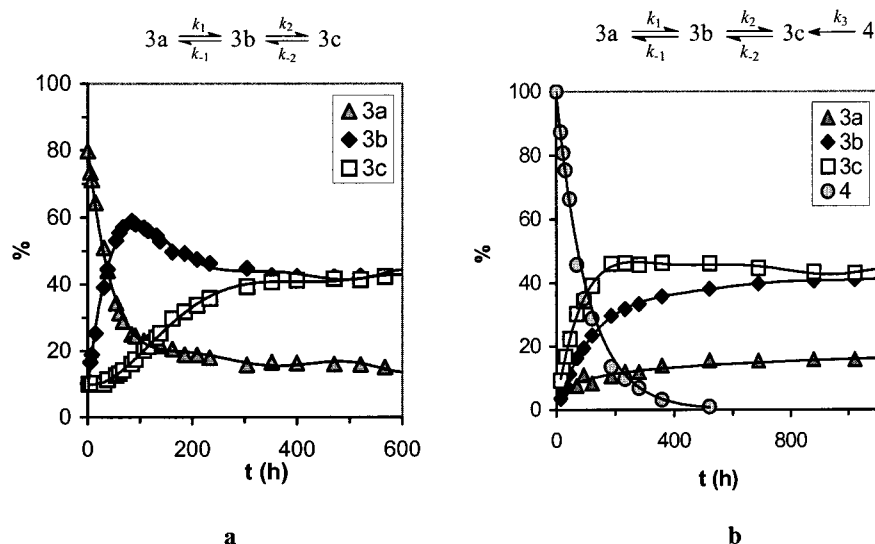


**Figure 5.** Isomerization at 76 °C of (a) a 8:1:1 mixture of **3a–c** and (b) **4** to the thermodynamically most stable mixture of **3a–c** (1:4:4 ratio).

energy of  $E_a = 117 \text{ kJ}\cdot\text{mol}^{-1}$  was obtained (Figure 6). Isomerization of the aluminosilsesquioxanes **3a–c** and **4** is relatively slow and gives the opportunity to study initially formed kinetic products as well as thermodynamically most stable products. Corresponding surface methyl aluminum species are likely to be even more thermally stable than **3a–c** and **4**, as their ligand environment is more rigid.

**Reactivity of Aluminosilsesquioxanes toward  $\text{Cp}_2\text{ZrX}_2$  ( $\text{X} = \text{Cl}, \text{Me}, \text{CH}_2\text{Ph}$ ).** Complexes **2–4** and **III** are realistic models for silica surface aluminum sites. Obviously, these aluminosilsesquioxanes are too simple to represent supported-MAO. Nevertheless, modified silicas might interact with the (pre)catalyst. Therefore, the reactivity of zirconocenes with aluminosilsesquioxane species was investigated.

It was argued that deprotonating the Brønsted acid **III** might afford a weakly coordinating anion supporting cationic metallocene species, in a fashion for example similar to that reported by Marks et al. for strongly

acidic sulfonated zirconia.<sup>16</sup> Reaction of  $\text{Cp}_2\text{ZrX}_2$  ( $\text{X} = \text{Me}, \text{CH}_2\text{Ph}$ ) with **III** in benzene- $d_6$  did not result in cationic zirconocene species. Instead, as assessed by  $^1\text{H}/^{13}\text{C}$  NMR spectral comparison with an authentic sample, a clean redistribution reaction was observed yielding  $[(c\text{-C}_5\text{H}_9)_7\text{Si}_7\text{O}_{11}(\text{OSiMePh}_2)]\text{ZrCp}_2$  (**5**) and various aluminum methyl species, which underlines the high oxophilicity of zirconium and the relatively weak aluminum–siloxide bonds in **III** (Scheme 4).<sup>10c,17</sup> When carried out in the presence of ethylene, no polymerization was observed and **5** was the only product formed, indicating that coordination of the silsesquioxane to zirconium is rapid and irreversible.<sup>18</sup> Comparable facile silsesquioxane transfer was observed for reactions of neutral zirconium alkyls with silsesquioxane-borato complexes.<sup>10c</sup>

The molecular structure of **5** (Figure 7) supports the presence of two inequivalent cyclopentadienyl groups, as was found in the  $^1\text{H}$  ( $\delta$  6.05, 6.02 ppm) and  $^{13}\text{C}$  ( $\delta$

(16) Ahn, H.; Marks, T. J. *J. Am. Chem. Soc.* **1998**, *120*, 13533–13534.

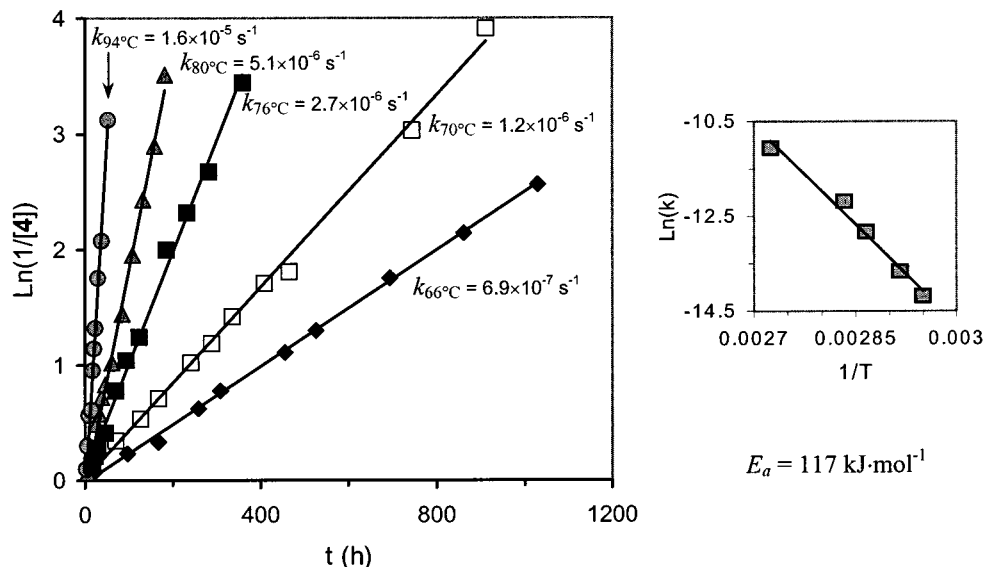


**Figure 6.** First-order and Arrhenius plots of isomerization of **4** into **3a–c**.

**Scheme 4. Reactivity of  $\text{Cp}_2\text{ZrMe}_2$  toward Aluminosilsesquioxane III**

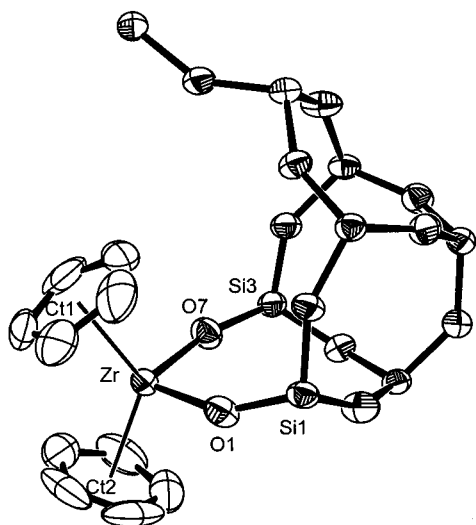
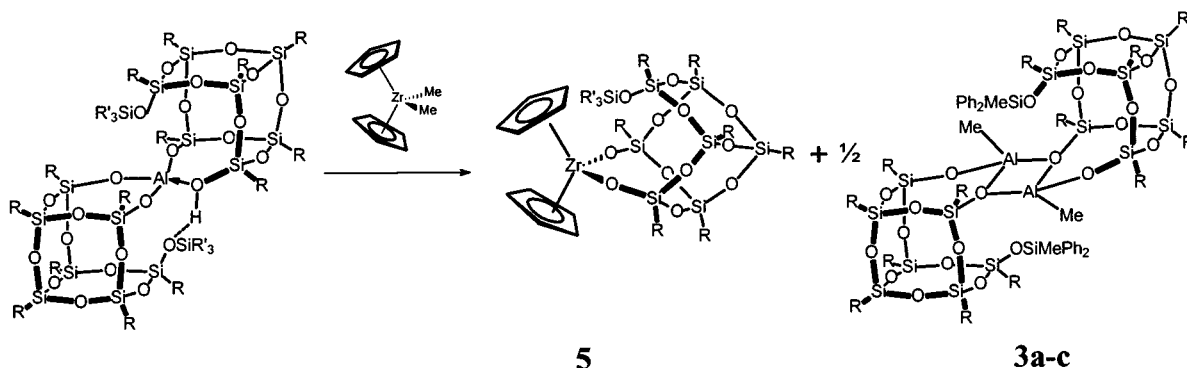


**Figure 7.** ORTEP drawing of the molecular structure of  $[(c\text{-C}_5\text{H}_9)_7\text{Si}_7\text{O}_{11}(\text{OSiMePh}_2)\text{ZrCp}_2]$  (**5**). Hydrocarbyl substituents on silicon are omitted for clarity. Thermal ellipsoids are scaled at the 50% probability level.

114.18, 113.49 ppm) NMR spectra of **5**. The Zr–O bond lengths (Table 1) are comparable to the  $\sigma\text{-Zr-O}$  distances in the zirconium silsesquioxane complexes  $[(c\text{-C}_6\text{H}_{11})_7\text{Si}_7\text{O}_{12}]\text{ZrCp}^*$  (1.96(3) Å),<sup>19</sup>  $[(c\text{-C}_5\text{H}_9)_7\text{Si}_7\text{O}_{11}(\text{OSiMe}_3)_2\text{Zr}\cdot\text{THF}_2$  (2.000(5) Å),<sup>10a</sup> and  $\{[(c\text{-C}_5\text{H}_9)_7\text{Si}_7\text{O}_{12}]\text{ZrCH}_2\text{-Ph}\}_2$  (1.958(5) Å).<sup>10a</sup>

Whereas no reaction seems to occur with **1** and **2**,  $\text{Cp}_2\text{ZrMe}_2$  definitely interacts with the Lewis acidic aluminosilsesquioxanes **3a–c** and **4**. In the presence of  $\text{Cp}_2\text{ZrMe}_2$ , benzene- $d_6$  solutions of **3a–c** and **4** equilibrate over 2 orders of magnitude faster than without  $\text{Cp}_2\text{ZrMe}_2$  (76 °C: **3a–c**, 1.5 h; **4**, 8 h; Figure 8). A similar result was obtained when **3a** was treated with  $\text{Cp}_2\text{Zr}(\text{CH}_2\text{Ph})_2$  (equilibration time 11 h, 76 °C). With an equilibration time of 180 h at 76 °C, the effect of  $\text{Cp}_2\text{ZrCl}_2$  on the equilibration rate of **3a–c** proved less dramatic. Worth mentioning is the fact that no methyl–benzyl or methyl–chloride exchange was observed between aluminum and zirconium ( $\text{Cp}_2\text{ZrX}_2$ , X = Cl,  $\text{CH}_2\text{Ph}$ ). Isomerization experiments with  $\text{Cp}_2\text{Zr}(\text{CD}_3)_2$  did not convincingly show exchange of  $\text{CH}_3$  and  $\text{CD}_3$  substituents between zirconium and aluminum either.

Clearly, the reaction rates  $k_1/k_{-1}$  and  $k_2/k_{-2}$  (Figures 5, 8) are significantly increased when  $\text{Cp}_2\text{ZrX}_2$  (X = Me,  $\text{CH}_2\text{Ph}$ , Cl) is added. It can be assumed that the aluminosilsesquioxanes **3a–c** and the zirconocene are in rapid equilibrium with a zwitterionic complex, similar to that found with  $\text{B}(\text{C}_6\text{F}_5)_3$  (Scheme 5).<sup>20</sup> However, since

(17) Sun, Y.; Metz, M. V.; Stern, C. L.; Marks, T. J. *Organometallics* **2000**, *19*, 1625–1627.

(18) Toluene, 10  $\mu\text{mol}$  Zr, 20  $\mu\text{mol}$  Al, 5 atm ethylene, 15 min at 25 °C, then heated to 80 °C for 15 min.

(19) Feher, F. J.; *J. Am. Chem. Soc.* **1986**, *108*, 3850–3852.



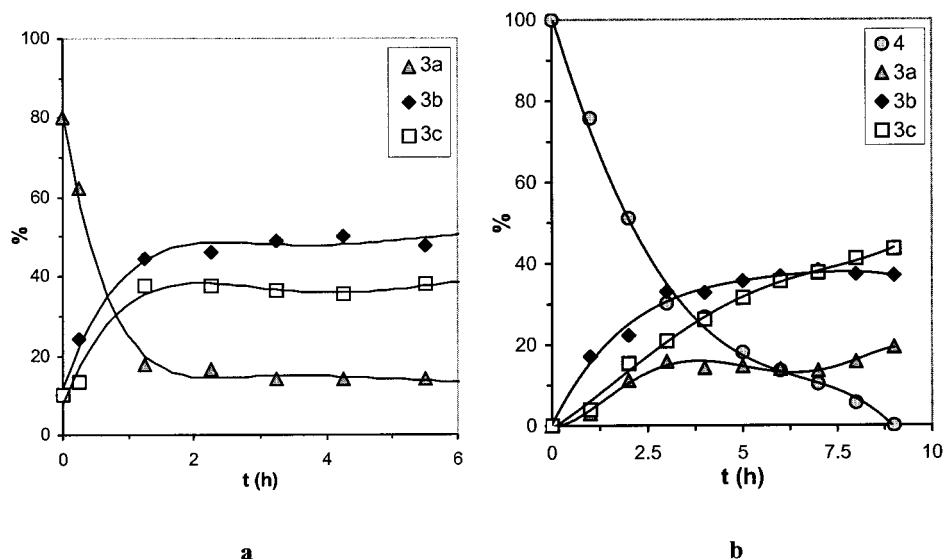
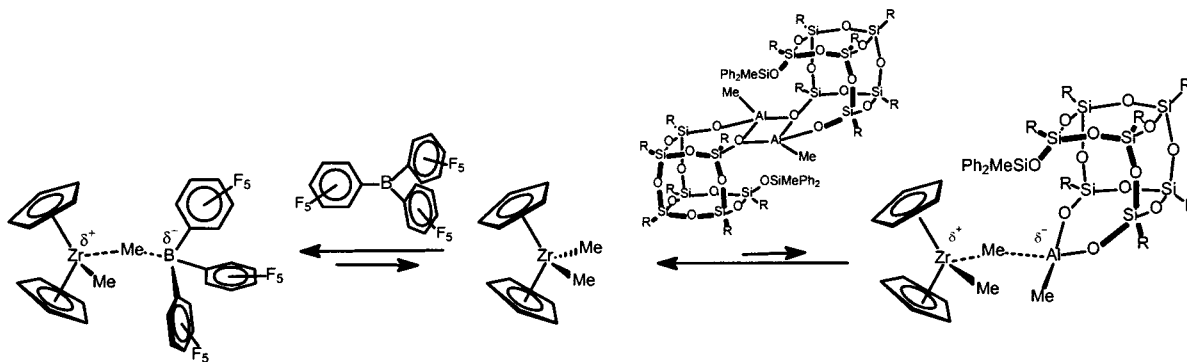


**Figure 8.** Isomerization of (a) a 8:1:1 mixture of **3a–c** and (b) **4** to the thermodynamically most stable mixture of **3a–c** (1:4:4 ratio) at 76 °C in the presence of an equimolar amount of  $\text{Cp}_2\text{ZrMe}_2$ .

**Scheme 5. Interaction of  $\text{Cp}_2\text{ZrMe}_2$  with  $\text{B}(\text{C}_6\text{F}_5)_3$  and **3a–c****



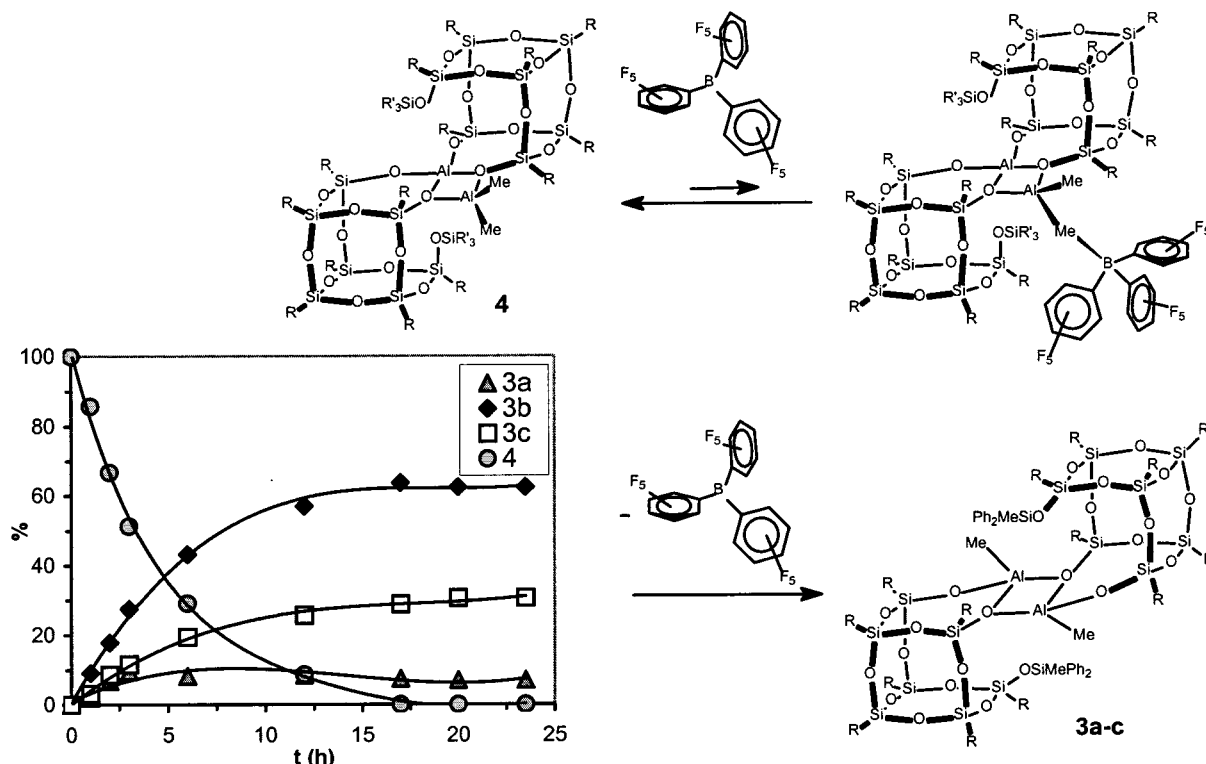
the NMR spectrum of an equimolar mixture of  $\text{Cp}_2\text{ZrX}_2$  and **3a–c** did not show any cationic or zwitterionic zirconocene-aluminate species, the equilibrium constant for the interaction between  $\text{Cp}_2\text{ZrX}_2$  and **3a–c** is small,  $K_{\text{eq}} < 0.03$ . This strongly suggests that **3a–c** and **4** are weaker Lewis acids than for example  $\text{B}(\text{C}_6\text{F}_5)_3$ ,  $[(t\text{-Bu})\text{-Al}(\mu_3\text{-O})]_n$  ( $n = 6, 7, 9$ ),<sup>21</sup> and MAO, which effectively abstract a methyl substituent from  $\text{Cp}_2\text{ZrMe}_2$  yielding an active ethylene polymerization catalyst. The inability of  $\text{B}(\text{C}_6\text{F}_5)_3$  to abstract methyl groups from **3a–c** and **4** indicates that the latter are not much less Lewis acidic than  $\text{B}(\text{C}_6\text{F}_5)_3$ , as this borane is known to abstract methyl groups even from fairly strong Lewis acidic compounds.<sup>20b,e–g</sup> Curiously, in the presence of  $\text{B}(\text{C}_6\text{F}_5)_3$  the isomerization of **4** into **3a–c** is accelerated over 2 orders of magnitude (20 h at 76 °C, Scheme 6). As soon as all of **4** has been converted, isomerization of the thus obtained kinetic mixture of **3a–c** (**3a:3b:3c** ratio = 1:9:4.4) is retarded to its original rate, indicating that the borane does not interact with **3a–c**. This demonstrates that the isomerization rate of **3a–c** is affected by Lewis bases only, while for **4** both Lewis acids and Lewis bases accelerate the isomerization.

**Concluding Remarks**

Even with the relatively simple model structures used in this study a variety of complexes is formed that can

convert into each other at elevated temperatures. The aluminosilsesquioxane complexes described here are interesting models for silica surface aluminum sites and provide insight into the complexity, mobility, and stability of silica-grafted aluminum alkyl species. Complexes **III** and **4** are probably the most realistic models for both Brønsted and Lewis acidic aluminum sites that can be formed during grafting of TMA onto hydroxylated silica surfaces.

A clear disadvantage of models of silica-supported complexes is their homogeneous nature, which allows them to aggregate to thermodynamically stable products with relatively low Lewis acidity. For example, these aluminosilsesquioxane complexes lack the latent<sup>21</sup> Lewis acidity necessary to effectively abstract a methyl group from  $\text{Cp}_2\text{ZrMe}_2$  to form an active olefin polymerization catalyst.<sup>20,21</sup> Nevertheless, the Lewis acidic complexes **3a–c** and **4** definitely interact with the weak Lewis basic  $\text{Cp}_2\text{ZrX}_2$  ( $\text{X} = \text{Me}, \text{CH}_2\text{Ph}, \text{Cl}$ ). Depending on the substituent X, the zirconocene can accelerate the isomerization of **3a–c** and **4** over 2 orders of magnitude. Surprisingly, complex **4** also reacts with the strongly Lewis acidic  $\text{B}(\text{C}_6\text{F}_5)_3$ . As soon as all **4** has been converted into **3a–c**, the accelerating effect stops, which demonstrates that Lewis acids have no effect on the isomerization of **3a–c**, suggesting that **3a–c** are stronger Lewis acids than **4**.

**Scheme 6. Isomerization of 4 into 3a–c in the Presence of B(C<sub>6</sub>F<sub>5</sub>)<sub>3</sub>**

### Experimental Section

**General Comments.** All manipulations were performed under an argon atmosphere using glovebox (Braun MB-150 GI) and Schlenk techniques. Solvents were distilled from Na (toluene) or Na/K alloy (hexanes) and stored under argon. NMR solvents were dried over Na/K alloy (benzene-*d*<sub>6</sub>) or 4 Å molecular sieves (toluene-*d*<sub>6</sub>). NMR spectra were recorded on a Varian Mercury 400 (<sup>1</sup>H, <sup>13</sup>C NMR, 25 °C) and Varian Indigo 500 (<sup>29</sup>Si NMR, 25 °C) spectrometers. Chemical shifts are reported in ppm and referenced to residual solvent resonances (<sup>1</sup>H, <sup>13</sup>C NMR) or external standards (<sup>29</sup>Si: SiMe<sub>4</sub> = 0 ppm). Elemental analyses were carried out at the Analytical Department of the University of Groningen (The Netherlands). Silsesquioxanes (c-C<sub>5</sub>H<sub>9</sub>)<sub>7</sub>Si<sub>8</sub>O<sub>12</sub>(OH) and (c-C<sub>5</sub>H<sub>9</sub>)<sub>7</sub>Si<sub>7</sub>O<sub>9</sub>(OH)<sub>2</sub>-OSiMePh<sub>2</sub> and aluminosilsesquioxane **III** were prepared following literature procedures.<sup>10b,e</sup>

**[(c-C<sub>5</sub>H<sub>9</sub>)<sub>7</sub>Si<sub>8</sub>O<sub>13</sub>]AlMe<sub>2</sub> (1a).** To a cooled (−90 °C) toluene (20 mL) solution of **I** (1.52 g, 1.66 mmol) was added AlMe<sub>3</sub> (0.83 mL, 2 M solution in *n*-heptane, 1.66 mmol). The mixture was slowly warmed to room temperature, upon which gas evolved and a gel formed. After filtration and drying, **1a** was isolated as a white powder (1.20 g, 1.23 mmol, 74%). <sup>1</sup>H NMR (benzene-*d*<sub>6</sub>, δ): 1.68 (m, 56H, CH<sub>2</sub>-C<sub>5</sub>H<sub>9</sub>), 1.24 (m, 7H, CH-C<sub>5</sub>H<sub>9</sub>), −0.13 (s, 6H, AlCH<sub>3</sub>). <sup>13</sup>C{<sup>1</sup>H} NMR (benzene-*d*<sub>6</sub>, δ): 27.62, 27.59, 27.57, 27.29 (CH<sub>2</sub>-C<sub>5</sub>H<sub>9</sub>), 22.47, 22.34, 22.27 (CH-C<sub>5</sub>H<sub>9</sub>, 1:3:3 ratio), −9.31 (AlCH<sub>3</sub>). <sup>29</sup>Si NMR (benzene-*d*<sub>6</sub>, δ): −64.74, −65.74 ((=O)<sub>3</sub>SiC<sub>5</sub>H<sub>9</sub>, 3:4 ratio), −102.66 ((=O)<sub>4</sub>Si). Anal. Calcd (found) for C<sub>37</sub>H<sub>69</sub>AlO<sub>13</sub>Si<sub>8</sub>: C, 45.64 (45.26); H, 7.14 (7.01).

**[(c-C<sub>5</sub>H<sub>9</sub>)<sub>7</sub>Si<sub>8</sub>O<sub>13</sub>]AlMe<sub>2</sub>Py (1b).** A suspension of **1a** (1.33 g, 1.37 mmol) in hexane (10 mL) was reacted with pyridine (0.2 mL, 2.5 mmol) at room temperature. Gradually **1a** reacted, forming a clear hexane solution from which **1b** could be isolated as fine colorless needles (0.78 g, 0.74 mmol, 54%). <sup>1</sup>H NMR (benzene-*d*<sub>6</sub>, δ): 8.41 (s, CH-py), 6.76 (s, CH-py), 6.49 (s, CH-py), 1.94 (m, 14H, CH<sub>2</sub>-C<sub>5</sub>H<sub>9</sub>), 1.80 (m, 14H, CH<sub>2</sub>-C<sub>5</sub>H<sub>9</sub>), 1.68 (m, 14H, CH<sub>2</sub>-C<sub>5</sub>H<sub>9</sub>), 1.51 (m, 14H, CH<sub>2</sub>-C<sub>5</sub>H<sub>9</sub>), 1.23 (m, 7H, CH-C<sub>5</sub>H<sub>9</sub>), −0.25 (s, 6H, AlCH<sub>3</sub>). <sup>13</sup>C{<sup>1</sup>H} NMR (benzene-*d*<sub>6</sub>, δ): 147.32 (CH-py), 139.22 (CH-py), 124.62 (CH-

py), 27.85, 27.79, 27.38, 27.31 (CH-C<sub>5</sub>H<sub>9</sub>), 22.97, 22.86, 22.80 (CH-C<sub>5</sub>H<sub>9</sub>, 3:1:3 ratio), −9.03 (br s, AlCH<sub>3</sub>). <sup>29</sup>Si NMR (benzene-*d*<sub>6</sub>, δ): −65.71, −65.78 ((=O)<sub>3</sub>SiC<sub>5</sub>H<sub>9</sub>, 3:4 ratio), −106.66 ((=O)<sub>4</sub>Si). Anal. Calcd (found) for C<sub>42</sub>H<sub>74</sub>AlNO<sub>13</sub>Si<sub>8</sub>: C, 47.92 (47.39); H, 7.09 (7.14).

**[(c-C<sub>5</sub>H<sub>9</sub>)<sub>7</sub>Si<sub>7</sub>O<sub>11</sub>(OSiMePh<sub>2</sub>)](AlMe<sub>2</sub>)<sub>2</sub> (2).** To a cooled (−80 °C) toluene solution (10 mL) of AlMe<sub>3</sub> (1.0 mL, 2 M in *n*-heptane, 2.0 mmol) was slowly added a solution of **II** (2.14 g, 200 mmol) in toluene (10 mL). The resulting mixture was stirred for 1 h at −80 °C, then slowly warmed to room temperature. The volatiles were evaporated, leaving a white foam. To remove traces of toluene, the foam was dissolved in hexane and subsequently dried in a vacuum to dryness, yielding (2.18 g) a crude mixture containing **2**, **3a–c**, and **III**. Slow crystallization gave colorless crystals of analytically pure **2** (0.22 g, 0.1 mmol, 9%). The <sup>1</sup>H NMR spectrum of the product obtained after evaporation of the mother liquor showed the presence of **3a–c** and the Brønsted acid **III**. <sup>1</sup>H NMR (benzene-*d*<sub>6</sub>, δ): 7.90 (dd, 4H, C<sub>6</sub>H<sub>5</sub>, <sup>3</sup>J<sub>HH</sub> = 8.0 Hz, <sup>4</sup>J<sub>HH</sub> = 1.4 Hz), 7.30 (t, 4H, C<sub>6</sub>H<sub>5</sub>, <sup>3</sup>J<sub>HH</sub> = 7.3 Hz), 7.21 (tt, 2H, C<sub>6</sub>H<sub>5</sub>, <sup>3</sup>J<sub>HH</sub> = 7.3 Hz, <sup>4</sup>J<sub>HH</sub> = 1.3 Hz), 1.8 (m, 56H, CH<sub>2</sub>-C<sub>5</sub>H<sub>9</sub>), 1.22 (m, 7H, CH-C<sub>5</sub>H<sub>9</sub>), 1.01 (s, 3H, SiCH<sub>3</sub>), −0.03 (s, 12H, AlCH<sub>3</sub>). <sup>13</sup>C{<sup>1</sup>H} NMR (benzene-*d*<sub>6</sub>, δ): 137.47, 134.72, 129.90, 127.96 (C<sub>6</sub>H<sub>5</sub>), 28.49, 28.20, 28.17, 28.11, 28.07, 28.02, 27.76, 27.30, 27.24, 27.15, 27.10, 27.01, 26.82 (CH<sub>2</sub>-C<sub>5</sub>H<sub>9</sub>), 25.93, 25.19, 24.57, 24.29, 23.09 (CH-C<sub>5</sub>H<sub>9</sub>, 1:2:2:1:1 ratio) 1.61 (SiCH<sub>3</sub>), −6.28 (AlCH<sub>3</sub>). <sup>29</sup>Si NMR (benzene-*d*<sub>6</sub>, δ): −10.77 (OSiMePh<sub>2</sub>), −60.29, −65.89, −66.04, −66.75, −67.00 ((=O)<sub>3</sub>SiC<sub>5</sub>H<sub>9</sub>, 2:2:1:1:1 ratio). Anal. Calcd (found) for C<sub>52</sub>H<sub>88</sub>Al<sub>2</sub>O<sub>12</sub>Si<sub>8</sub>: C, 52.75 (53.46); H, 7.49 (7.73).

**[(c-C<sub>5</sub>H<sub>9</sub>)<sub>7</sub>Si<sub>7</sub>O<sub>11</sub>(OSiMePh<sub>2</sub>)]AlMe<sub>2</sub> (3a–c).** AlMe<sub>3</sub> (1.15 mL, 2 M in heptane, 2.30 mmol) was added to a cooled (−80 °C) toluene solution (30 mL) of **II** (2.46 g, 2.29 mmol). The mixture was allowed to slowly warm to room temperature. The solvent was evaporated, and the crude product was dissolved in hexane and subsequently dried in a vacuum. This procedure was repeated until a nonsticky solid was obtained. The <sup>1</sup>H NMR spectrum of the crude product showed a mixture of isomers of **3a–c** with a molar ratio **3a:3b:3c** = 35:55:10. The

**Table 2. Details of the X-ray Structure Determination of  $\{[(c-C_5H_9)_7Si_7O_{11}(OSiMePh_2)](AlMe_2)_2\}_2$  (**2**),  $\{[(c-C_5H_9)_7Si_7O_{11}(OSiMePh_2)]AlMe_2\}_2$  (**3a/3c**),  $[(c-C_5H_9)_7Si_7O_{11}(OSiMePh_2)]_2Al_2Me_2$  (**4**), and  $[(c-C_5H_9)_7Si_7O_{11}(OSiMePh_2)]ZrCp_2$  (**5**)**

	<b>2</b>	<b>3a</b>	<b>3c</b>	<b>4</b>	<b>5</b>
formula	C <sub>104</sub> H <sub>176</sub> Al <sub>4</sub> O <sub>24</sub> Si <sub>16</sub> ·(C <sub>6</sub> H <sub>14</sub> )	C <sub>98</sub> H <sub>158</sub> Al <sub>2</sub> O <sub>24</sub> Si <sub>16</sub>	C <sub>98</sub> H <sub>158</sub> Al <sub>2</sub> O <sub>24</sub> Si <sub>16</sub>	C <sub>98</sub> H <sub>158</sub> Al <sub>2</sub> O <sub>24</sub> Si <sub>16</sub>	C <sub>58</sub> H <sub>86</sub> O <sub>12</sub> Si <sub>8</sub> Zr
fw	2453.98	2223.64	2223.64	2223.64	1291.21
cryst syst	monoclinic	triclinic	triclinic	monoclinic	monoclinic
space group, no.	<i>P</i> 2 <sub>1</sub> / <i>n</i>	<i>P</i> 1	<i>P</i> 1	<i>C</i> 2/ <i>c</i>	<i>P</i> 2 <sub>1</sub> / <i>c</i>
<i>a</i> , Å	14.151(2)	13.211(9)	13.2074(16)	35.013(3)	14.133(5)
<i>b</i> , Å	20.858(3)	14.624(9)	14.5633(17)	12.524(1)	21.400(5)
<i>c</i> , Å	22.798(3)	16.518(9)	16.748(2)	28.329(3)	22.386(5)
$\alpha$ , deg		81.86(1)	82.022(2)		
$\beta$ , deg	96.391(3)	89.90(2)	88.659(2)	104.449(2)	107.07(2)
$\gamma$ , deg		71.15(1)	70.444(3)		
<i>V</i> , Å <sup>3</sup>	6687(2)	2986(4)	3005.2(6)	12030(2)	6472(3)
<i>D</i> <sub>calc</sub> , g cm <sup>-3</sup>	1.219	1.1236	1.229	1.228	1.325
<i>Z</i>	2	1	1	4	4
<i>F</i> (000), electrons	2636	1188	1188	4752	2728
$\mu$ (Mo, K $\alpha$ ), cm <sup>-1</sup>	2.4	2.49	2.47	2.47	2.47
cryst size, mm	0.4 × 0.2 × 0.2	0.1 × 0.1 × 0.1	0.10 × 0.05 × 0.05	0.2 × 0.2 × 0.1	0.2 × 0.2 × 0.2
<i>T</i> , K	236(2)	236(2)	203(2)	236(2)	203(2)
$\theta$ range, deg:	1.33, 26.37	1.63, 20.82	1.50, 20.82	1.47, 28.29	1.51, 26.37
min, max					
$\lambda$ (Mo, K $\alpha$ ), Å	0.71073	0.71073	0.71073	0.71073	0.71073
monochromator	graphite	graphite	graphite	graphite	graphite
index ranges	<i>h</i> : -17→17 <i>k</i> : 0→26 <i>l</i> : 0→28	<i>h</i> : -13→13 <i>k</i> : -14→14 <i>l</i> : 0→16	<i>h</i> : -13→13 <i>k</i> : -14→14 <i>l</i> : 0→16	<i>h</i> : -34→33 <i>k</i> : 0→12 <i>l</i> : 0→12	<i>h</i> : -17→16 <i>k</i> : 0→26 <i>l</i> : 0→27
tot. no. of data	52 651	23 416	19 196	47 607	35 543
unique data	13 659	6256	6289	6301	13 207
<i>wR</i> ( <i>F</i> <sup>2</sup> )	0.1422	0.2642	0.1576	0.2232	0.0775
<i>R</i> ( <i>F</i> )	0.0552	0.0955	0.0709	0.0809	0.0408
Goof	1.074	1.079	1.022	1.024	1.062
largest diff peak, hole, e/Å <sup>3</sup>	0.534, -0.431	0.688, -0.503	0.423, -0.336	0.539, -0.424	0.426, -0.448

mixture was fractionally crystallized from hexane, yielding five fractions of crystals of **3a–c** with variable molar ratios of the isomers **3a–c** (1.15 g, 0.52 mmol, 45%). Repeated crystallization gave single crystals of **3a** and **3c** suitable for an X-ray structure determination. The remaining mother liquor consisted mainly (90%) of **3b**. Anal. Calcd (found) for C<sub>49</sub>H<sub>79</sub>AlO<sub>12</sub>Si<sub>8</sub>: C, 52.93 (51.53); H, 7.16 (7.06). **3a**: <sup>1</sup>H NMR (benzene-*d*<sub>6</sub>,  $\delta$ ): 7.80 (m, 8H, C<sub>6</sub>H<sub>5</sub>), 7.25 (m, 12H, C<sub>6</sub>H<sub>5</sub>), 1.68 (br m, 112H, CH<sub>2</sub>-C<sub>5</sub>H<sub>9</sub>), 1.18 (m, 14H, CH-C<sub>5</sub>H<sub>9</sub>), 0.94 (s, 6H, SiCH<sub>3</sub>), -0.23 (s, 6H, AlCH<sub>3</sub>). <sup>13</sup>C{<sup>1</sup>H} NMR (benzene-*d*<sub>6</sub>,  $\delta$ ): 138.15, 137.57, 134.69, 134.60, 129.72, 129.61, 127.84, 127.80 (C<sub>6</sub>H<sub>5</sub>), 28.08, 28.05, 27.99, 27.95, 27.90, 27.85, 27.78, 27.71, 27.64, 27.49, 27.45, 27.42, 27.35, 27.32, 27.22, 27.20, 27.18, 27.13 (CH<sub>2</sub>-C<sub>5</sub>H<sub>9</sub>), 25.09, 24.13, 23.88, 23.65, 22.89, 22.82 (CH-C<sub>5</sub>H<sub>9</sub>, 1:1:1:2:1:1 ratio), 0.15 (SiCH<sub>3</sub>), -11.87 (AlCH<sub>3</sub>). <sup>29</sup>Si NMR (benzene-*d*<sub>6</sub>,  $\delta$ ): -10.20 (OSiMePh<sub>2</sub>), -56.70, -64.76, -64.95, -66.66, -67.09 ((=O)<sub>3</sub>SiC<sub>5</sub>H<sub>9</sub>, 2:1:1:1:2 ratio). **3b**: <sup>1</sup>H NMR (benzene-*d*<sub>6</sub>,  $\delta$ ): 7.82 (m, 8H, C<sub>6</sub>H<sub>5</sub>), 7.32 (m, 12H, C<sub>6</sub>H<sub>5</sub>), 1.68 (br m, 112H, CH<sub>2</sub>-C<sub>5</sub>H<sub>9</sub>), 1.2 (m, 14H, CH-C<sub>5</sub>H<sub>9</sub>), 1.04 (s, 3H, SiCH<sub>3</sub>), 0.94 (s, 3H, SiCH<sub>3</sub>), -0.08 (s, 3H, AlCH<sub>3</sub>), -0.10 (s, 3H, AlCH<sub>3</sub>). <sup>13</sup>C{<sup>1</sup>H} NMR (benzene-*d*<sub>6</sub>,  $\delta$ ): 138.29, 138.05, 137.88, 137.80, 134.92, 134.75, 134.69, 129.67, 129.62, 127.99, 127.78 (C<sub>6</sub>H<sub>5</sub>), 29.30, 28.79, 28.74, 28.55, 28.45, 28.32, 28.17, 28.02, 27.93, 27.90, 27.81, 27.79, 27.77, 27.61, 27.54, 27.50, 27.45, 27.42, 27.36, 27.31, 27.25, 27.21 (CH<sub>2</sub>-C<sub>5</sub>H<sub>9</sub>), 25.16, 24.85, 24.79, 24.72, 24.13, 24.06, 24.04, 23.31, 22.91, 22.87, 22.83, 22.78 (CH-C<sub>5</sub>H<sub>9</sub>, 1:1:1:1:1:1:2:1:1:2:1 ratio), 0.58, -0.18 (SiCH<sub>3</sub>), -11.28, -11.89 (AlCH<sub>3</sub>). <sup>29</sup>Si NMR (benzene-*d*<sub>6</sub>,  $\delta$ ): -9.75, -10.37 (OSiMePh<sub>2</sub>), -57.77, -61.01, -62.61, -63.39, -64.13, -64.24, -65.18, -65.21, -65.99, -66.60, -66.76, -66.93, -67.49 ((=O)<sub>3</sub>SiC<sub>5</sub>H<sub>9</sub>, 1:1:1:1:2:1:1:1:1:1:1:1 ratio). **3c**: <sup>1</sup>H NMR (benzene-*d*<sub>6</sub>,  $\delta$ ): 7.80 (m, 8H, C<sub>6</sub>H<sub>5</sub>), 7.25 (m, 12H, C<sub>6</sub>H<sub>5</sub>), 1.68 (br m, 112H, CH<sub>2</sub>-C<sub>5</sub>H<sub>9</sub>), 1.21 (m, 14H, CH-C<sub>5</sub>H<sub>9</sub>), 0.92 (s, 6H, SiCH<sub>3</sub>), -0.35 (s, 6H, AlCH<sub>3</sub>). <sup>13</sup>C{<sup>1</sup>H} NMR (benzene-*d*<sub>6</sub>,  $\delta$ ): 138.22, 137.50, 134.72, 134.59, 129.71, 129.62, 127.79 (C<sub>6</sub>H<sub>5</sub>), 28.61, 28.51, 28.33, 27.99, 27.93, 27.90, 27.86, 27.82, 27.73, 27.63, 27.60, 27.50, 27.43, 27.39, 27.36, 27.22, 27.19, 27.13 (CH<sub>2</sub>-C<sub>5</sub>H<sub>9</sub>), 25.05, 24.68, 24.19, 23.77, 23.38, 22.92, 22.57 (CH-C<sub>5</sub>H<sub>9</sub>, 1:1:1:1:1:1:1 ratio), -0.12 (SiCH<sub>3</sub>), -11.78 (AlCH<sub>3</sub>). <sup>29</sup>Si NMR (benzene-*d*<sub>6</sub>,  $\delta$ ): -10.21 (OSiMePh<sub>2</sub>), -57.91, -63.95, -64.20, -64.90, -65.80, -66.52, -67.11 ((=O)<sub>3</sub>SiC<sub>5</sub>H<sub>9</sub>, 1:1:1:1:1:1:1 ratio).

**[(c-C<sub>5</sub>H<sub>9</sub>)<sub>7</sub>Si<sub>7</sub>O<sub>11</sub>(OSiMePh<sub>2</sub>)<sub>2</sub>Al<sub>2</sub>Me<sub>2</sub> (**4**)]**. To a toluene solution (7 mL) of AlMe<sub>3</sub> (0.5 mL, 2 M in *n*-heptane, 1 mmol) was slowly added a toluene solution (7 mL) of **III** (2.2 g, 1.0 mmol) at room temperature. The mixture was stirred for 1 h, then the volatiles were evaporated and the remaining foam was twice dissolved in hexane and evaporated to dryness. The crude product was recrystallized from hexane to yield **4** (1.77 g, 0.40 mmol, 79%) as colorless crystals. <sup>1</sup>H NMR (benzene-*d*<sub>6</sub>,  $\delta$ ): 7.81 (m, 8H, C<sub>6</sub>H<sub>5</sub>), 7.3 (m, 12H, C<sub>6</sub>H<sub>5</sub>), 1.65 (br m, 126H, C<sub>5</sub>H<sub>9</sub>), 0.86 (s, 6H, SiCH<sub>3</sub>), -0.24 (s, 6H, AlCH<sub>3</sub>). <sup>13</sup>C{<sup>1</sup>H} NMR (benzene-*d*<sub>6</sub>,  $\delta$ ): 137.99, 137.79, 134.74, 134.72, 129.66, 129.57, 127.93 (C<sub>6</sub>H<sub>5</sub>), 29.08, 28.76, 28.07, 27.98, 27.88, 27.86, 27.81, 27.74, 27.51, 27.45, 27.38, 27.23, 27.17, 27.14, 26.85 (CH<sub>2</sub>-C<sub>5</sub>H<sub>9</sub>), 25.51, 25.21, 24.09, 23.49, 23.00, 22.82, 22.66 (CH-C<sub>5</sub>H<sub>9</sub>, 1:1:1:1:1:1:1 ratio), 0.04 (SiCH<sub>3</sub>), -7.38 (AlCH<sub>3</sub>). <sup>29</sup>Si NMR (benzene-*d*<sub>6</sub>,  $\delta$ ): -10.77 (OSiMePh<sub>2</sub>), -60.92, -62.63, -63.77, -64.12, -65.38, -66.86, -66.94 ((=O)<sub>3</sub>SiC<sub>5</sub>H<sub>9</sub>, 1:1:1:1:1:1:1 ratio). Anal. Calcd (found) for C<sub>98</sub>H<sub>164</sub>O<sub>24</sub>Al<sub>2</sub>Si<sub>16</sub>: C, 52.93 (52.69); H, 7.16 (7.23).

**[(c-C<sub>5</sub>H<sub>9</sub>)<sub>7</sub>Si<sub>7</sub>O<sub>11</sub>(OSiMePh<sub>2</sub>)<sub>2</sub>ZrCp<sub>2</sub> (**5**)]**. (a) An NMR tube was charged with an equimolar amount of Cp<sub>2</sub>ZrMe<sub>2</sub> and **III**. Upon addition of benzene-*d*<sub>6</sub>, vigorous gas evolution was observed. The <sup>1</sup>H and <sup>13</sup>C showed **5** as the sole zirconocene complex present, as was proved by comparing the NMR spectra with those of **5** prepared by the following method. (b) To a stirred toluene solution (25 mL) of Cp<sub>2</sub>ZrCl<sub>2</sub> (1.18 g, 4.04 mmol) and (c-C<sub>5</sub>H<sub>9</sub>)<sub>7</sub>Si<sub>7</sub>O<sub>9</sub>(OH)<sub>2</sub>OSiMePh<sub>2</sub> (4.33 g, 4.04 mmol) was added NEt<sub>3</sub> (5 mL). Upon heating the mixture to reflux for 1 h, a white salt precipitated. The volatiles were evaporated, and the product was extracted with hexane (30 mL). Slow cooling of a saturated hexane solution yielded **5** as colorless block-shaped crystals (2.74 g, 2.12 mmol, 53%). Concentration and further cooling of the mother liquor yielded a second crop of **5** (1.10 g, 0.85 mmol, 21%) as a white microcrystalline material. <sup>1</sup>H NMR (benzene-*d*<sub>6</sub>,  $\delta$ ): 7.66 (m, 4H, Ar), 7.16 (m, 6H, Ar), 6.05 (s, 5H, C<sub>5</sub>H<sub>5</sub>), 6.02 (s, 5H, C<sub>5</sub>H<sub>5</sub>), 1.71 (bm, 56H, CH<sub>2</sub>-C<sub>5</sub>H<sub>9</sub>), 1.17 (m, 7H, CH-C<sub>5</sub>H<sub>9</sub>), 0.54 (s, Si(CH<sub>3</sub>)Ph<sub>2</sub>). <sup>13</sup>C{<sup>1</sup>H} NMR (benzene-*d*<sub>6</sub>,  $\delta$ ): 137.80 (*ipso*-C<sub>6</sub>H<sub>5</sub>), 134.57 (C<sub>6</sub>H<sub>5</sub>), 129.61 (C<sub>6</sub>H<sub>5</sub>), 127.78 (C<sub>6</sub>H<sub>5</sub>), 114.18 (C<sub>5</sub>H<sub>5</sub>), 113.49 (C<sub>5</sub>H<sub>5</sub>), 28.51, 28.36, 28.17, 28.11, 28.02, 27.95, 27.92, 27.59, 27.47, 27.45, 27.42, 27.23, 27.17 (CH<sub>2</sub>-C<sub>5</sub>H<sub>9</sub>), 25.29, 24.12, 24.06, 23.22, 23.14 (CH-C<sub>5</sub>H<sub>9</sub>, 1:2:2:1:1 ratio), -0.17 (CH<sub>3</sub>). <sup>29</sup>Si NMR

(benzene- $d_6$ ,  $\delta$ ): -11.37 (*S*MePh<sub>2</sub>), -64.52, -65.22, -65.63, -65.67, -67.06 ((=O)<sub>3</sub>SiC<sub>5</sub>H<sub>9</sub>, 1:2:1:1:2 ratio). Anal. Calcd (found) for C<sub>58</sub>H<sub>86</sub>O<sub>12</sub>Si<sub>8</sub>Zr: C, 53.95 (54.06); H, 6.71 (6.66).

**Isomerization of  $\{[(c-C_5H_9)_7Si_7O_{11}(OSiMePh_2)]AlMe\}_2$  (**3a-c**).** For this study NMR tubes were charged with solutions of **3a-c** (ratio **3a:3b:3c** = 8:1:1) in benzene- $d_6$  (60 mM), sealed, and heated at 76 °C. At set time intervals, the <sup>1</sup>H NMR spectrum of the sample was recorded and the ratio of **3a-c** determined. The reaction was followed until the thermodynamic equilibrium was reached.

**Kinetic Studies on Isomerization of  $[(c-C_5H_9)_7Si_7O_{11}(OSiMePh_2)]_2Al_2Me_2$  (**4**).** For this study NMR tubes were charged with solutions of **4** in benzene- $d_6$  (30–60 mM), sealed, and heated at a constant temperature of 76 °C. At set time intervals, the <sup>1</sup>H NMR spectrum of the sample was recorded and the decay of **4** determined (**4** to **5** half-life times  $t_{1/2}$ ). The rate constants (*k*) at four different temperatures were used to determine the activation energy  $E_a$  ( $R^2 = 0.984$ ), which was found to be 117 kJ·mol<sup>-1</sup>.

**Isomerization of  $\{[(c-C_5H_9)_7Si_7O_{11}(OSiMePh_2)]AlMe\}_2$  (**3a-c**) and  $[(c-C_5H_9)_7Si_7O_{11}(OSiMePh_2)]_2Al_2Me_2$  (**4**) in the Presence of Cp<sub>2</sub>ZrX<sub>2</sub> (X = Me, CH<sub>2</sub>Ph, Cl) or B(C<sub>6</sub>F<sub>5</sub>)<sub>3</sub>.** NMR tubes were charged with solutions of **3a-c** (ratio **3a:3b:3c** = 8:1:1) or **4** in benzene- $d_6$  (60 mM), sealed, and heated at 76 °C. At set time intervals, the <sup>1</sup>H NMR spectrum of the sample was recorded and the ratio of **4** and **3a-c** determined. The reaction was followed until the thermodynamic equilibrium was reached.

**X-ray Structure Determination of **2**, **3a**, **3c**, **4**, and **5**.** Suitable crystals were selected, mounted on a thin, glass fiber using paraffin oil, and cooled to the data collection temperature. Data were collected on a Bruker AX SMART 1k CCD diffractometer using 0.3°  $\omega$ -scans at 0°, 90°, and 180° in  $\phi$ . Unit-cell parameters were determined from 60 data frames collected at different sections of the Ewald sphere. Semiempirical absorption corrections based on equivalent reflections

were applied.<sup>22</sup> No symmetry higher than triclinic was observed for **3a** and **3c**. Systematic absences in the diffraction data are consistent for *Cc* and *C2/c* for **4** and uniquely consistent for the reported space group for **2** and **5**. Solution in the centric options yielded chemically reasonable and computationally stable results of refinement. The structures were solved by direct methods, completed with difference Fourier syntheses, and refined with full-matrix least-squares procedures based on  $F^2$ . All non-hydrogen atoms were refined with anisotropic displacement parameters. All hydrogen atoms were treated as idealized contributions. All scattering factors and anomalous dispersion factors are contained in the SHEX-TL 5.10 program library.<sup>23</sup> Selected bond distances and angles are given in Table 1, and detailed data are listed in Table 2.

**Acknowledgment.** The Dutch Polymer Institute and the Schuit Institute of Catalysis are gratefully acknowledged for financing this work.

**Supporting Information Available:** Full listings of crystallographic data, atomic parameters, hydrogen parameters, atomic coordinates, bond distances, and bond angles for **2**, **3a**, **3b**, **4**, and **5**. This material is available free of charge via the Internet at <http://pubs.acs.org>.

OM0102596

(20) (a) Yang, X.; Stern, C. L.; Marks, T. J. *J. Am. Chem. Soc.* **1994**, *116*, 10015–10031. (b) Bochmann, M.; Dawson, D. M. *Angew. Chem., Int. Ed. Engl.* **1996**, *35*, 2226–2228. (c) Coles, M. P.; Jordan, R. F. *J. Am. Chem. Soc.* **1997**, *119*, 8125–8126. (d) Amor, F.; Butt, A.; du Plooy, K. E.; Spaniol, T. P.; Okuda, J. *Organometallics* **1998**, *17*, 5836–5849. (e) Song, X.; Thornton-Pett, M.; Bochmann, M. *Organometallics* **1998**, *17*, 1004–1006. (f) Green, M. L. H.; Sassmannhausen, J. *Chem. Commun.* **1999**, 115–116. (g) Guérin, F.; Stephan, D. W. *Angew. Chem., Int. Ed.* **2000**, *39*, 1298–1300.

(21) For example see: (a) Harlan, C. J.; Bott, S. G.; Barron, A. R. *J. Am. Chem. Soc.* **1995**, *117*, 6465–6474. (b) Koide, Y.; Bott, S. G.; Barron, A. R. *Organometallics* **1996**, *15*, 2213–2226.

(22) Blessing, R. *Acta Crystallogr.* **1995**, *A51*, 33.

(23) Scheldrick, G. M. *SHELXT*; Bruker AXS: Madison, WI, 1997.